105 (2026) 106818

Contents lists available at ScienceDirect

Poultry Science

journal homepage: www.elsevier.com/locate/psj

Protein co-expression network analysis explores biological mechanisms associated with meat quality variability in broilers affected by breast myopathies: A focus on wooden breast

Martina Bordini [a], Massimiliano Petracci [a], Francesca Soglia [a,*], Shai Barbut [b]

[a] Department of Agricultural and Food Sciences, Alma Mater Studiorum University of Bologna, Piazza Goidanich 60, Cesena, FC 47521, Italy
[b] Department of Food Science, University of Guelph, Ontario, Canada

ARTICLE INFO

Keywords:
TMT-based proteomics
Co-expression network
Pectoralis major muscle
White striping
Spaghetti meat

ABSTRACT

Growth-related myopathies affecting fast-growing broilers still represent a challenge for the poultry industry, and the need for comprehensive and additional knowledge useful to mitigate the occurrence of these myopathies persists. This study aimed at exploring the association between the proteome profiles and the meat quality traits (i.e., weight, morphometric parameters, pHu, color, and compression force) of broiler breast fillets affected by the white striping (WS), wooden breast (WB), and spaghetti meat (SM), as well as the normal ones (NB), by applying the WGCNA approach ($N = 12$). The co-expression network analysis detected 10 color-coded modules of co-expressed proteins significantly correlated with the meat quality traits, particularly characterizing the WB defect in terms of meat quality differences, and thus leading to a focus on this specific myopathy for data interpretation. The brown, turquoise, green, and black modules were significantly correlated with at least three of the phenotypic traits and thus considered for further investigations. The outcomes were largely in accordance with a wealth of literature regarding transcriptomic and proteomic characterizations of breast muscles affected by these myopathies, evidencing proteins entering these modules enriched with terms involved in mitochondrial and antioxidant activities, as well as collagen composition and extracellular matrix organization. Furthermore, based on the results gained through the protein co-expression analysis, different roles between fibrillar and non-fibrillar collagens in the characterization of the WB condition have been hypothesized, as well as an impairment of the molecular processes involved in protein synthesis and quality-control, mainly regarding the eIF3 complex.

Introduction

According to the scientific and industry literature, broiler breast myopathies known as white striping (**WS**), wooden breast (**WB**), and spaghetti meat (**SM**) still present remarkable challenges for the poultry meat industry (Barbut et al., 2024). As recently reviewed by Greene et al. (2025a), despite the big efforts in gathering knowledge regarding their causative mechanisms to help identifying strategies to mitigate their prevalence and severity, as well as carrying out in-depth characterizations of these conditions from physiological and molecular points of view (Papah et al., 2018; Lake et al., 2021; Soglia et al., 2021; Alnahhas et al., 2023; Wang et al., 2025), the understanding of their etiologies remains limited while their incidence levels are still rising (Greene et al., 2025a). This can predominantly be due to the complexity of factors associated with their occurrence and progression, as demonstrated by numerous studies published in the past decade (Bailey et al., 2015, 2020; Che et al., 2022; Bordignon et al., 2022; Bailey, 2023; Barbut et al., 2024; Wang et al., 2025), which considered these myopathies as complex and multi-factorial conditions. These studies highlight the need for additional investigations, which could assist in identifying new and improved strategies to mitigate the occurrence of these myopathies.

Prepared for submission to
POULTRY SCIENCE
Full-Length Article
Section: Molecular and Cellular Biology
* Corresponding author.
E-mail address: francesca.soglia2@unibo.it (F. Soglia).

https://doi.org/10.1016/j.psj.2026.106818
Received 23 December 2025; Accepted 17 March 2026
Available online 18 March 2026

Different omics approaches have been recently used to study complex physiological phenotypes, as well as pathological conditions in humans/animals, among which genomics, transcriptomics, proteomics, and metabolomics have been the most widely applied (Karczewski and Snyder, 2018; Zhou et al., 2025). This has become possible due to outstanding progress in high-throughput technologies that have helped boost the exploration of underlying mechanisms of intricate phenotypes and conditions. At the same time, powerful bioinformatic strategies were developed to transform information into data formats easier to apply and helpful in understanding cellular and molecular pathways underlying the biological systems under study (Pei et al., 2017; Nice, 2022; Rosati et al., 2024). In this context, tandem mass tagging (**TMT**)-based proteomics, a high-throughput mass spectrometry (**MS**)-based proteomic approach, provides quantitative measurement of proteins, enabling the outlining of the proteome profiles of specific phenotypic conditions (Du et al., 2021; Nice, 2022; Dang et al., 2022; Zhou et al., 2025). As bioinformatic tools to interpret proteomic data, network-focused approaches represent valuable strategies to investigate the expression patterns of proteins of a particular tissue and obtain a picture of cellular responses as complete as possible. Numerous studies have recently applied the Weighted Gene Co-Expression Network Analysis (**WGCNA**) as a bioinformatic approach to interpret and explore high-throughput data, such as transcriptomic, proteomic, and metabolomic data in several research fields (Pei et al., 2017; Zhang et al., 2018; Oulas et al., 2019; Zhou et al., 2024; Wei et al., 2024). Among these, WGCNA has already been used to explore high-throughput microarray and RNA-seq datasets obtained to investigate the cellular and biological mechanisms underlying the onset of broiler breast myopathies (Pampouille et al., 2019; Bordini et al., 2021, 2022; Wang et al., 2023a). Recently, researchers investigated human diseases by applying WGCNA with proteomic datasets and achieved insights into proteome profile changes associated with the condition under study (Li et al., 2024).

In our present study, the aim was to explore potential interactions between meat quality traits and proteomic profiles of *Pectoralis major* muscles in broilers affected by growth-related myopathies, based on the hypothesis of distinct patterns of protein expression between affected and unaffected samples, and the potential use of protein network analysis to detect groups of co-expressed proteins associated with the variability of phenotypic traits characterizing myopathic fillets. For this we employed the above-mentioned "WGCNA" approach (in R environment) to identify networks of co-expressed proteins in muscles affected by WS, WB, and SM as well as in their unaffected counterpart - control (normal breast; **NB**), potentially revealing the dysregulation of pathways and processes in affected samples and thus providing additional insights into the pathogenic mechanisms of myopathies.

Materials and methods

Experimental design and sample collection

Eighty samples (20/group) of skinless breast fillets belonging to the same flock of fast-growing broilers (Aviagen Ross 708; 2.5 kg live weight) were collected at a commercial processing plant in Ontario, Canada, and classified based on their macroscopic features as normal (NB) and severely affected by WS, WB, or SM. Single fillets macroscopic classification of each myopathy was performed by the same members of the research team, following the criteria proposed by Barbut et al. (2024).

Meat quality evaluation and sample selection

Each fillet brought to the University of Guelph meat laboratory was measured to evaluate the morphometric measurements (i.e., fillet weight, length, width, and height), as well as ultimate pH (pHu), lightness (L*), redness (a*), yellowness (b*), and hardness (by a 20% compression force test) at 24 h post-mortem. The cranial part of each breast fillet surface was used to measure the pHu and color, respectively by using a pH meter (HI 98163, Hanna Instruments, Woonsocket, RI) and a colorimeter (Chroma Meter CR-400; Konica Minolta, Mississauga, ON, Canada). A compression force test was performed as previously described by Wang et al. (2023b). To investigate proteome changes characterizing chicken *Pectoralis major* muscles affected by WS, WB, and SM myopathies, three samples per group were chosen to be submitted to proteomic analysis. Overall, samples have been selected by considering the macroscopic classification of each myopathy and textural characteristics, specifically by considering samples with the highest hardness (measured as compression force described above) for WB group and lower hardness for the others (i.e., WS, SM, and NB), and taking the ones with the highest degree of severity according to the classification reviewed by in Barbut et al. (2024) for each specific myopathy (with no signs ascribable to other myopathies).

Sample preparation for proteomics and quality control

One gram from each sample was used to extract proteins for proteome analysis by TMT-based mass spectrometry. Briefly, samples were analyzed for 12-plex TMT-based mass spectrometry analysis (Thermo Fisher Center for Multiplexed Proteomics facility at the Harvard Medical School). The 12-plex experiment was designed to contain 3 samples per group (NB, WS, WB, and SM). Sample digestion, TMT labeling, TMT-based mass spectrometry, as well as protein annotation and quantification were performed at the same proteomic center. Specifically, mass spectra were searched using the COMET algorithm against a Chicken Proteome downloaded from UniProt (Bateman et al., 2025) in both forward and reverse directions and considering contaminating protein sequences. For each annotated protein, the corresponding gene symbol was reported in the proteomic dataset. Searches were performed using a peptide mass tolerance of 50 ppm, and a fragment ion tolerance of 0.4 ppm. Peptide spectral matches were filtered to a 1% false discovery rate (**FDR**) using the target-decoy strategy combined with linear discriminant analysis. The proteins were filtered to $a < 1\%$ FDR and quantified only from peptides with a summed signal-to-noise threshold of > 180. Protein quantitation was performed by summing the signal-to-noise values for all peptides for a given protein. Each TMT channel was summed across all quantified proteins and normalized to enforce equal protein loading. Each protein's quantitative measurement was then scaled to 100 to obtain a normalized relative abundance.

Protein co-expression network analysis

Normalized relative abundance of proteins quantified by at least two peptides and detected in at least 2 of the 3 samples per each experimental group were considered for the subsequent bioinformatic analysis. Overall, the proteome profiles and the phenotypic data of the 12 samples selected for the proteomic analysis were used to perform the weighted co-expression network analysis ($N = 12$), using the "WGCNA" package (version 1.72-5) (Langfelder and Horvath, 2008) in R environment (version 4.3.2; R Core Team, 2020). We acknowledge potential limitations of this study related to the sample size. In any case, according to the recommendation from developers for somewhat small dataset (<20 samples), the following aspects have been considered to implement the co-expression network analysis and outlier detection, as well as to verify that our network adheres to an appropriate scale-free topology in order to ensure reliability of our dataset (Langfelder and Horvath, 2008; Horvath, 2011). Briefly, the construction of unsigned weighted co-expression networks was achieved by using the normalized proteomic profile of each sample with no missing values. In particular, the gene symbols referring to each protein, entering the proteome dataset, have been used to create an adjacency matrix in which the nodes correspond to the normalized relative abundance of each protein, and the edges are represented by their pairwise Pearson's correlation (Langfelder and

Horvath, 2008). To establish the adjacency matrix, an appropriate soft threshold power (β value) of 9 was chosen, applying the approximate scale-free topology criterion. Briefly, according to the developers' instructions for small dataset, this value was chosen as the scale-free topology index (R^2) reached the peak ($R^2 > 0.90$) for the first time when $\beta = 9$. Then, the protein network was constructed using the *blockwiseModules* function, and groups of co-expressed proteins (i.e., modules) were detected by employing the Dynamic Tree Cut algorithm (Langfelder and Horvath, 2008) and choosing 2 for the DeepSplit parameter and 30 for the minimum module size in the *blockwiseModules* function. Afterward, to detect the group of co-expressed proteins most significantly related to the meat quality evaluation and morphometric measures of WS, WB, SM and NB, we investigated correlations between module eigenproteins (**ME**) and phenotypic traits. More in detail, once the modules have been detected and identified as color-coded labels, the ME of each group has been calculated using the principal component analysis criterion (Langfelder and Horvath, 2008). This allowed us to assess the relationship between modules and traits by using the ME as a weighted average expression level of each module and thus used to identify the "module-trait association" as the means of Pearson's correlation between every ME and external trait. Benjamini-Hochberg FDR has been considered as adjusted *P* value. For each selected module, the software calculated the protein significance (**PS**), which corresponds to the correlation value between each phenotype and protein expression level, as well as the module membership (i.e., the intramodular connectivity) of each protein belonging to a specific module (Langfelder and Horvath, 2008).

Protein modules selection

Our investigation focused on modules significantly correlated with at least three of the phenotypic traits considered for the present study. More specifically, we decided to consider for further analysis the turquoise, brown, green, and black modules to point out the most relevant functional terms enriched with these protein expression patterns.

Functional annotation of co-expressed proteins

The lists of gene symbols referring to each protein entering the modules selected for further analysis were individually used to perform two different functional enrichment analyses. First, ClueGO v2.5.5 (Bindea et al., 2009), a Cytoscape software 3.10.2 plugin (Shannon et al., 1971) allowing to gain biological information for large lists of genes or proteins (Mlecnik et al., 2018), was used to perform the functional characterization of the selected protein modules (i.e., brown, turquoise, green, and black) by the using UniProt-GOA Database for Gene Ontology (**GO**) functional annotation. Also, the ClueGo plugin enabled us to explore how functional terms are interconnected with each other by displaying an "annotation network" of color-coded functional terms based on the term-term similarity. More in detail, the term-term similarity was calculated using the corrected *kappa* statistic, which determines the association strength between the terms (Bindea et al., 2009). A Benjamini-Hochberg FDR adjusted $P < 0.05$ was chosen as the threshold for significance.

Secondly, an additional functional enrichment analysis was performed using the Database for Annotation, Visualization and Integrated Discovery (DAVID Knowledgebase v2024q4) (Huang et al., 2008; Sherman et al., 2022) to understand the biological meaning and functional grouping of the proteins entering the modules most significantly related to the considered phenotypic traits. The list of gene symbols referring to each protein belonging to the modules selected for functional analyses has been individually analyzed using the Functional Annotation Clustering tool. Biological Processes (**BP**), Molecular Function (**MF**), and Cellular Components (**CC**) have been considered as GO term categories included in the DAVID Knowledgebase for functional characterization. For this analysis, a Benjamini-Hochberg FDR was used to adjust *P* values. Enriched GO terms with FDR-adjusted $P < 0.05$ were considered statistically significant. Also, FDR-adjusted $P < 0.01$ was considered as the threshold to identify the most significant functional categories.

Homo sapiens background was used as the reference organism for both DAVID and Cytoscape enrichment analyses.

Western blot analysis

Considering the specific focus on the WB defect, three target collagen proteins, the fibrillar Collagen type III (i.e., Collagen type III alpha 1 chain; COL3A1) and those composing the non-fibrillar Collagen type IV (i.e., Collagen type IV alpha 1 and 2 chains; COL4A1 and COL4A2), were chosen to validate and further investigate some of the results obtained in this study. Briefly, one gram of each frozen samples belonging to the WB and NB group ($n = 3$/group) was used to extract the insoluble protein fraction enriched in myofibrillar and structural proteins and perform western blot analysis following the procedure described by Soglia et al. (2022). In detail, a rabbit polyclonal anti-human COL4A1 (LS-C352029, LSBio, Lynnwood, WA; 1:4,000), a rabbit polyclonal anti-COL4A2 (Abcam, ab125208, Cambridge, UK; 1:4,000) and a rabbit anti-COL3A1 (Abcam, ab185659, Cambridge, UK; 1:4,000) primary antibodies were used. Final detection and densitometry differences were analyzed as described by Soglia et al. (2022). Considering NB group as reference, results were expressed as fold change of the normalized expression of each protein in WB.

Statistical analysis

Data elaboration and statistical analysis have been carried out in R environment (version 4.3.2). Specifically, the effect of WB, WS, and SM on the considered traits (i.e., morphometric measures of raw fillets, pHu, color, and compression force) have been statistically evaluated to assess differences between groups by one-way ANOVA. Thus, the "group" was considered as the main effect, and – when significant – mean values were separated via the parametric Tukey-HSD test. As for the western blot results, differences between the WB and NB samples in the expression of target proteins considered for validation were assessed by using a non-parametric t-test (Mann-Whitney U-test), due to the small number of replicates per group. Overall, differences were considered statistically significant at a P value < 0.05.

Results

Meat quality evaluation

The effects of WS, WB, and SM myopathies on fillet weight and morphometric measurements (fillet length, height, and width), pHu, color (L*, a*, and b*) and compression force are reported in Table 1.

Proteomic profiles of the Pectoralis major muscles

From TMT-based mass spectrometry, 4,199 proteins were quantified and mapped to the *Gallus gallus* Uniprot database. Since only proteins identified by at least 2 peptides were considered for downstream analysis, the normalized relative abundance of 3,277 proteins was used to construct the co-expression networks. As the first step into the co-expression network analysis, the normalized proteomic dataset, with no missing values, has been used to cluster the samples and potentially identify outliers (Figure 1). Overall, no outliers were found. Also, results from sample clustering based on their proteomic profiles showed that samples clustered according to the experimental group to which they belonged.

Table 1
Effects of broiler breast myopathies (NB = Normal Breast; WS = White Striping; WB = Wooden Breast; SM = Spaghetti Meat) for different raw fillets parameters (N = 80; 20 muscles/experimental group) tested by one-way ANOVA. Tukey-HSD test was carried out to separate the means ($P < 0.05$).

	NB	WS	WB	SM	*P* value
Fillet weight (g)	173.90 ± 5.23c	270.34 ± 7.20b	313.55 ± 8.24a	294.55 ± 10.63ab	***
Fillet length (cm)	15.33 ± 0.20b	16.61 ± 0.19a	16.88 ± 0.17a	16.98 ± 0.17a	***
Fillet width (cm)	8.65 ± 0.12b	9.88 ± 0.16a	9.53 ± 0.20a	9.90 ± 0.14a	***
Fillet height (cm)	2.53 ± 0.07c	3.48 ± 0.07b	4.05 ± 0.09a	3.48 ± 0.10b	***
pHu	5.74 ± 0.03b	5.75 ± 0.03b	6.04 ± 0.05a	5.76 ± 0.04b	***
Lightness (L*)	51.82 ± 0.58b	51.86 ± 0.55b	56.06 ± 0.57a	53.53 ± 0.43b	***
Redness (a*)	1.36 ± 0.24b	2.23 ± 0.27a	1.52 ± 0.16b	1.99 ± 0.25ab	*
Yellowness (b*)	2.98 ± 0.45cd	5.83 ± 0.43a	4.17 ± 0.43bc	5.29 ± 0.26ab	***
Compression force (N)	2.32 ± 0.22b	3.98 ± 0.42b	12.11 ± 0.99a	3.51 ± 0.27b	***

[a-d] : Mean value ± SE followed by different letters in each row are significantly different.
*** = $P \leq 0.001$.
* = $P \leq 0.05$.

Protein co-expression network analysis

The protein co-expression network was constructed using the normalized TMT-based proteomic datasets of the 12 fillets selected for proteomics with no missing values and the corresponding phenotypic traits of raw fillets (i.e., weight, morphometric parameters, pHu, color, and compression force). To construct the network, we first found the optimal soft-thresholding power (β) to transform the co-expression similarity into the adjacency matrix by performing the analysis of network topology for several soft-thresholding parameters. Figure 2**A** reports the β estimated through the function *pickSoftThreshold* in the WGCNA package. A power of 9 was chosen, based on the first time β reached a scale-free topology index at peak ($R^2 > 0.90$). Once the network had been constructed by the software (Figure 2**B**), the analysis revealed a total of 10 color-coded modules of co-expressed proteins that ranged in size from 1,797 (i.e., turquoise module) to 45 (i.e., magenta module) proteins.

The identification of biologically significant modules and proteins/genes is one of the major goals of co-expression analysis. In this regard, the WGCNA R package enables users to quantify correlation values between each protein module and the considered phenotype (Langfelder and Horvath, 2008), thus assessing the module-trait association. To do so, once the groups of proteins characterized by a similar trend of expression (i.e. modules named using different color labels) have been identified, the ME of each module was calculated using the principal component analysis criterion. This allowed us to calculate Pearson's correlations between each ME and trait, and thus to identify the module-trait relationship. Correlations between ME and phenotypic traits evidenced that four modules were significantly related ($P < 0.05$) to breast weight (i.e., brown, blue, turquoise, and black), three modules to compression force (i.e., turquoise, green, and black), two modules to breast length (i.e., grey and brown), five modules to breast height (i.e., brown, blue, turquoise, green, and black), three modules to the pHu (i.e., turquoise, green, and black), and one module was significantly related to yellowness (b*) (i.e., grey). As shown by the heatmap (Figure 3), several traits share the same significantly associated groups of co-expressed proteins, which are characterized by different strengths and directions in terms of correlation values.

Because of the high amount of data obtained through WGCNA in

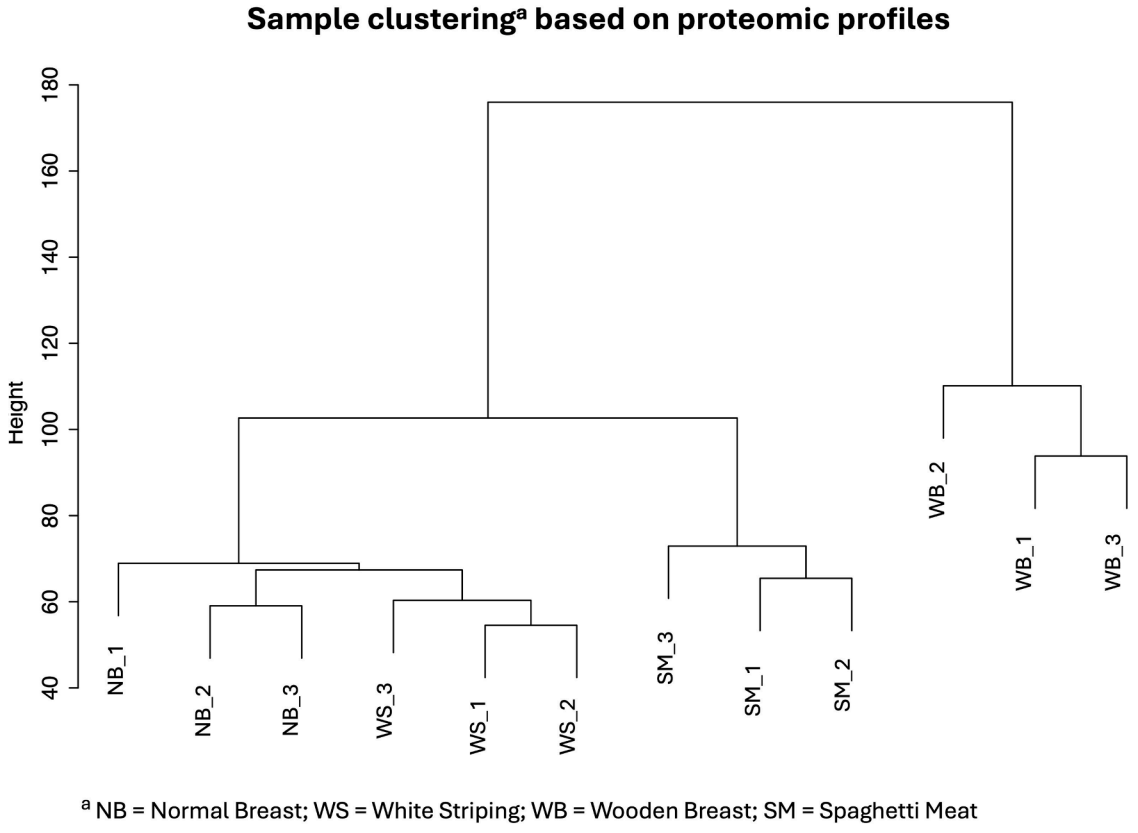

Fig. 1. Sample clustering based on the *Pectoralis major* muscles' proteomic profiles.

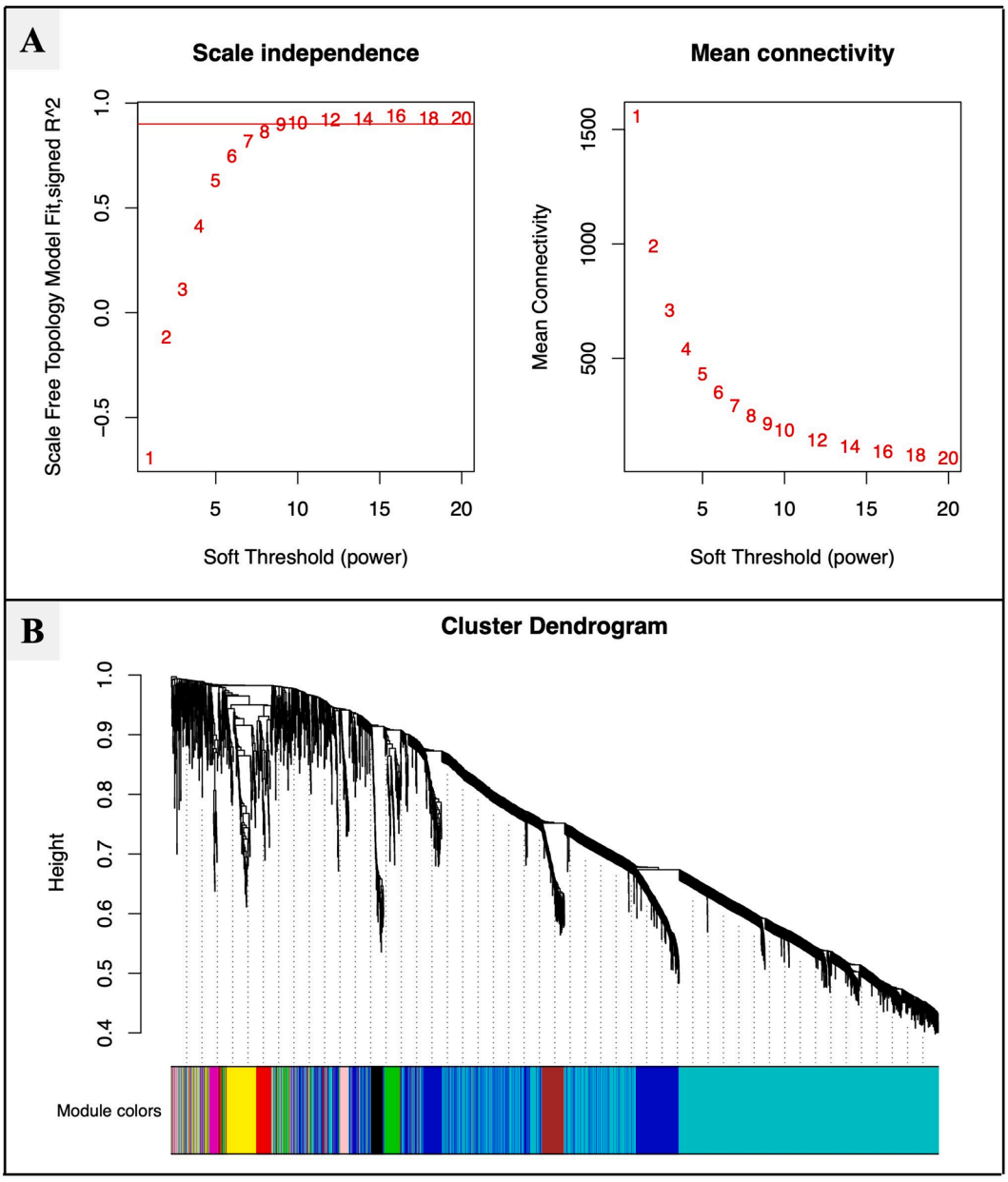

Fig. 2. Protein co-expression network construction. Panel A: Analysis of network topology for several soft-thresholding powers: the left graph shows the scale-free fit index as a function of the soft-thresholding power, right graph displays the mean connectivity as a function of the soft-thresholding power. Panel B: Clustering dendrogram of the samples' protein expression profiles to construct the network of co-expression and identify modules. The figure shows the cluster dendrogram of 3,277 proteins considered for this analysis. Each branch in the figure represents one protein, and every color below represents the corresponding co-expression module.

terms of protein expression patterns associated with the traits of interest, we decided to focus our attention on modules significantly related with at least three of the considered phenotypic traits. Therefore, the brown, turquoise, green, and black modules, which respectively include 192, 1,797, 115, and 70 proteins were considered. Among those, only the turquoise module showed a positive correlation with the traits of interest. More specifically, the turquoise module was positively related ($P < 0.01$) to breast weight and height (+0.82 and +0.90, respectively), as well as to compression force of the fillets and pHu (+0.86 and +0.64, respectively). On the other hand, the brown module was negatively related to fillet weight (−0.87; $P < 0.001$), width (−0.68; $P < 0.05$), and height (−0.77; $P < 0.01$). The green module was negatively related to compression force (−0.75; $P < 0.01$), fillet height (−0.61; $P < 0.05$), and pHu (−0.59; $P < 0.05$), while the black module was negatively related to fillet weight (−0.65; $P < 0.05$), fillet height (−0.78; $P < 0.001$), compression force (−0.66; $P < 0.05$), and pHu (−0.68; $P < 0.05$). Table 2 reports all the correlation values between each module and trait. It is worth noting that all the considered traits showed significant differences among the experimental groups (WS, WB, SM, and NB), thus allowing us to explore the differences in the proteome profiles in relation to the phenotypic variability of quality and morphological traits measured in normal and myopathic fillets. However, the results allowed us to specifically characterize the WB samples, but not the WS and SM groups. This is particularly evident when considering the significantly higher values of fillet height, pHu, L*, and compression force of WB samples compared to all the other groups (Table 1). Also, sample clustering based on the *Pectoralis major* muscles' proteomic profiles clearly showed differences between the WB and the other groups, thus reinforcing the discussion focused on protein expression patterns characterizing this condition.

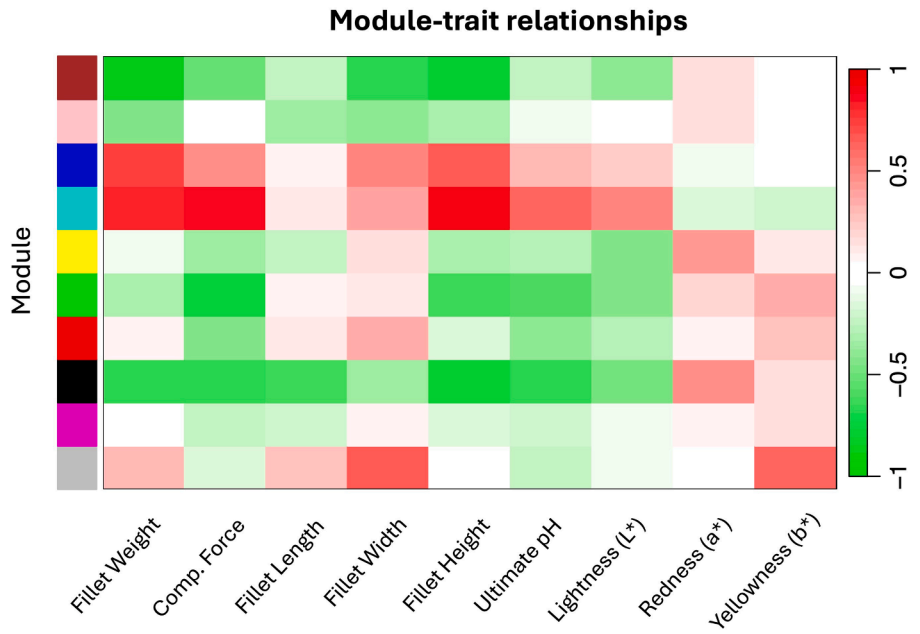

Fig. 3. Module-trait relationships. The heatmap shows associations between modules and meat quality and morphometric traits measured for each sample: fillet weight, fillet length, fillet width, fillet height, ultimate pH, lightness (L*), redness (a*), yellowness (b*), and compression force (Comp. Force). Traits are reported on the x-axis, and modules are reported on the y-axis. The heatmap is color-coded by correlation values: green represents a negative correlation, while red represents a positive correlation.

Table 2
Pearson's correlation values between the color-coded modules (module eigenprotein values) and the quality traits of *Pectoralis major* muscles included in the present study: fillet weight, compression force, fillet length, width and height, ultimate pH (pHu), lightness (L*), redness (a*), and yellowness (b*). Benjamini-Hochberg FDR has been considered as adjusted *P* value. Protein modules are reported following the same order reported by the module-trait relationships heatmap in Figure 3. Significant values are shown in bold.

Modules	Fillet weight	Comp. Force	Fillet length	Fillet width	Fillet height	pHu	L*	a*	b*
Brown	**−0.87*****	−0.51	−0.22	**−0.68***	**−0.77****	−0.24	−0.38	+0.15	−0.04
Pink	−0.44	−0.03	−0.35	−0.41	−0.32	−0.08	−0.05	+0.16	−0.01
Blue	**+0.74****	+0.48	+0.09	+0.52	**+0.66***	+0.31	+0.25	−0.09	−0.02
Turquoise	**+0.82****	**+0.86*****	+0.10	+0.38	**+0.90*****	**+0.64***	+0.50	−0.16	−0.21
Yellow	−0.07	−0.35	−0.25	+0.14	−0.32	−0.27	−0.43	+0.43	+0.13
Green	−0.31	**−0.75****	+0.09	+0.12	**−0.61***	**−0.59***	−0.43	+0.19	+0.37
Red	+0.09	−0.44	+0.11	+0.37	−0.17	−0.38	−0.27	+0.07	+0.27
Black	**−0.65***	**−0.66***	**−0.62***	−0.36	**−0.78****	**−0.68***	−0.48	+0.47	+0.15
Magenta	+0.01	−0.25	−0.21	+0.06	−0.17	−0.22	−0.07	+0.09	+0.16
Grey	+0.31	−0.15	+0.28	**+0.65***	+0.02	−0.24	−0.08	−0.02	**+0.64***

*** = *P* value ≤ 0.001.
** = *P* value ≤ 0.01.
* = *P* value ≤ 0.05.

Functional analysis

Biological interpretations of protein modules selected for functional analysis were carried out by using both the ClueGO Cytoscape plug-in and DAVID Knowledgebase online tool. More in detail, lists of gene symbols referring to the proteins entering each selected module (i.e., brown, turquoise, green, and black) were individually submitted to DAVID and the ClueGO Cytoscape plugin to understand their biological meaning. These functional enrichment analyses allowed us to point out the most relevant functional terms associated with proteins entering the considered modules, which are significantly related to the phenotypic variability of the morphological measures and meat quality traits considered in the present study. Figures 4-7 display the annotation networks of GO terms clustered based on their term-term similarities (Bindea et al., 2009), and referring to the turquoise (Figure 4), brown (Figure 5), black (Figure 6), and green (Figure 7) modules. Tables 3-6 report the most significant functional terms (Benjamini-Hochberg FDR adjusted *P* value < 0.01) identified through the DAVID analysis by individually considering the lists of gene symbols encoding for proteins belonging to the turquoise (Table 3), brown (Table 4), black (Table 5), and green (Table 6) modules. Interestingly, both enrichment analyses identified "glycolytic process", "Arp2/3 complex-mediated actin nucleation", "cytoplasmic translational initiation" and "purine nucleotide biosynthetic process" as some of the most significant GO terms enriching the turquoise module, and thus positively related to the breast weight and height, compression force and pHu. As for the brown module, "mitochondrial electron transport, ubiquinol to cytochrome c", "cristae formation", "acetyl-CoA biosynthetic process from pyruvate", and "pyruvate dehydrogenase (NAD+) activity" were found as significant functional terms by both the functional annotation approaches. Similarly, functional analysis of proteins entering the black module evidenced terms related to "aerobic respiration", "mitochondrial electron transport, NADH to ubiquinone", "mitochondrial respiratory chain complex I assembly", "mitochondrial electron transport, cytochrome c

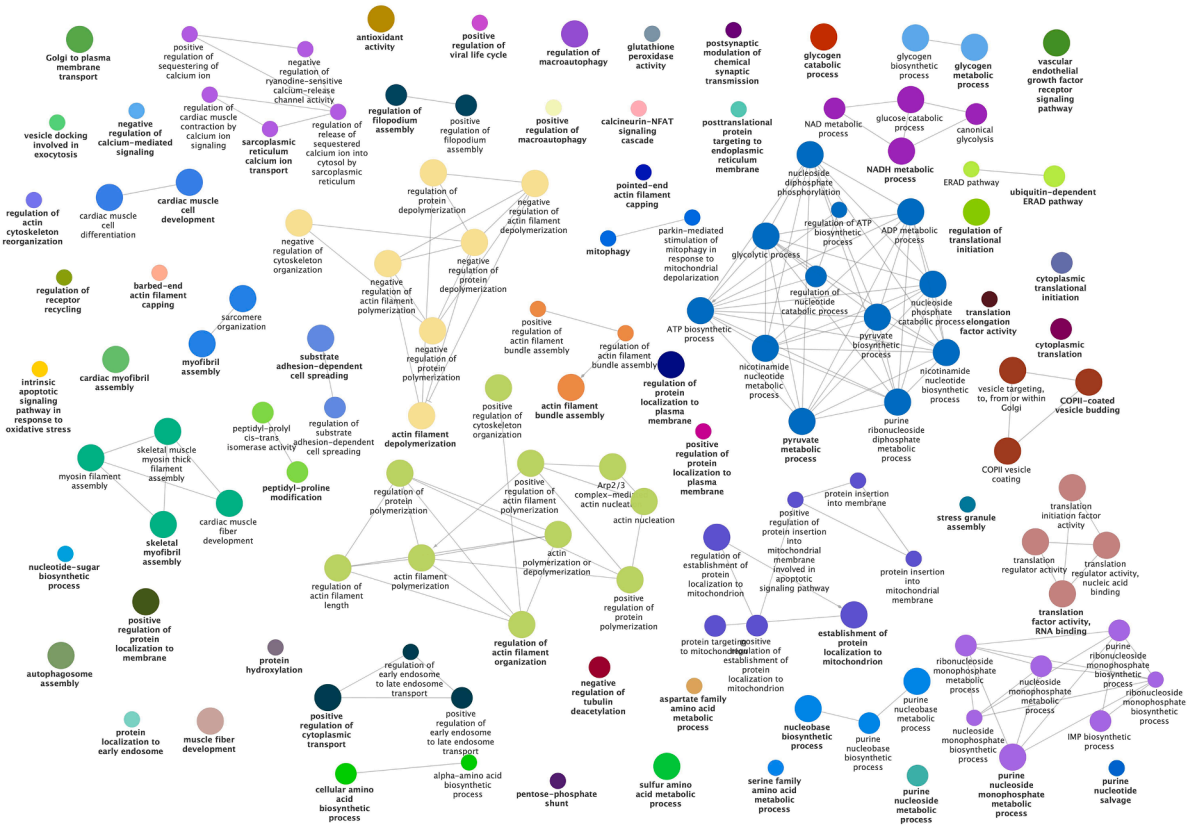

Fig. 4. ClueGO functional analysis of proteins belonging to the **turquoise** module. The figure shows the most significant GO terms (Biological Process) identified by the ClueGO Cytoscape plugin and how terms are grouped and interact with each other. Different groups of functional terms are distinguished by different colors. Terms displaying the same color belong to the same network of functional terms, based on the *kappa* statistics score: 0.7. Terms reported in bold indicate the leading group of each GO term (according to Benjamini-Hochberg FDR adjusted *P* value), while nodes size reflects the enrichment significance of the terms: terms having the biggest node size are the most significant ones.

to oxygen", "NADH dehydrogenase (ubiquinone) activity", and "cytochrome-c oxidase activity" by considering both the functional annotation approaches. Lastly, "formation of cytoplasmic translation initiation complex" and "translation initiation factor activity" were found by the ClueGO and DAVID analyses as functional GO terms enriching the green module. The comprehensive results obtained from the ClueGO and DAVID analyses are reported in Supplementary Tables S2 and S3, respectively.

Western blot analysis

Results of the target collagen proteins quantification in WB and NB groups carried out by western blot analysis are reported in Table 7. Bands having a molecular weight of 114, 119, and 116 kDa, respectively ascribed to the COL3A1, COL4A1, and COL4A2 native proteins, were detected. Compared to NB, a tendency of higher COL3A1 expression (FC = 1.51; $P = 0.08$), as well as of lower COL4A2 abundance (FC = 0.52; $P = 0.08$) was found in WB. On the other hand, results showed no differences in the COL4A1 normalized expression between the groups.

Discussion

Over the past decades, significant advancements in high-throughput technologies have provided researchers with outstanding opportunities to explore the regulatory mechanisms underlying complex traits and diseases in humans and animal species. As an example, co-expression network analysis has emerged as a widely adopted and effective strategy for elucidating the molecular processes underlying both physiological functions and pathological conditions of traits/conditions under study. Indeed, this bioinformatic analysis has been proposed as a powerful tool to identify groups of co-expressed genes, proteins and metabolites (Pei et al., 2017) associated with specific traits or clinical features in humans and animal species (Zhang et al., 2018; Chen et al., 2021; Zhou et al., 2024; Wei et al., 2024).

In recent years, several studies have applied the WGCNA method to microarray and RNA-seq datasets to investigate gene expression patterns associated with the occurrence of broiler breast myopathies with the aim of elucidating the main molecular and cellular pathways associated with their occurrence (Pampouille et al., 2019; Bordini et al., 2021, 2022; Wang et al., 2023a). However, to the best of our knowledge, WGCNA using proteomic data has not been carried out yet to explore protein expression patterns associated with the occurrence of broiler myopathies. The present study thus aimed at exploring key modules (i.e., patterns of co-expressed proteins) significantly correlated with the phenotypic variability of meat quality traits substantially affected by the manifestation of WS, WB and SM myopathies (Table 2).

Following a similar approach used in previous studies (Bordini et al., 2021, 2022), it has been decided to assess the differences in the protein expression profiles in relation to the phenotypic variability of quality and morphological traits measured in normal and abnormal fillets (i.e., severely affected by WS, WB or SM). More specifically, WGCNA allowed us to investigate the proteome profiles of fillets affected and not affected by breast myopathies by identifying patterns of co-expressed proteins that were significantly correlated with the phenotypic variability of the considered traits. In this regard, it is now well-established that the occurrence of broiler myopathies, especially considering the WS and WB defects, is associated with the improved growth performance (e.g., fast growth-rate and hypertrophy of breast muscle) of modern broiler

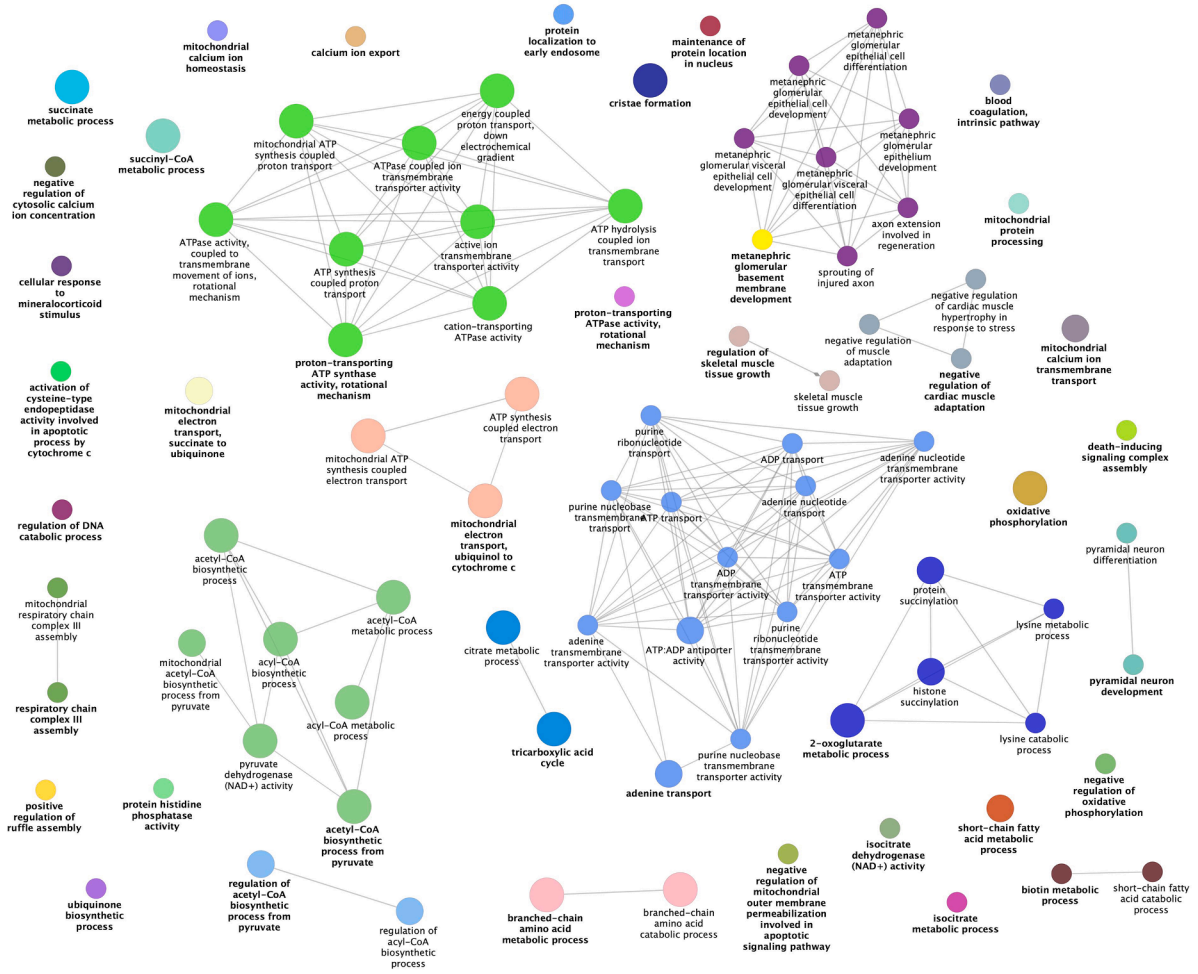

Fig. 5. ClueGO functional analysis of proteins belonging to the **brown** module. The figure shows the most significant GO terms (Biological Process) identified by the ClueGO Cytoscape plugin and how terms are grouped and interact with each other. Different groups of functional terms are distinguished by different colors. Terms displaying the same color belong to the same network of functional terms, based on the *kappa* statistics score: 0.7. Terms reported in bold indicate the leading group of each GO term (according to Benjamini-Hochberg FDR adjusted *P* value), while nodes size reflects the enrichment significance of the terms: terms having the biggest node size are the most significant ones.

hybrids (Barbut et al., 2024), which also implies associations between their occurrence and the morphometric measures such as fillet weight, length and thickness characterizing commercial fast-growing broilers. This was demonstrated by several studies showing an association between the severity of WB and WS and increased fillet thickness and weight (Petracci et al., 2019; Che et al., 2022). Moreover, breast myopathies manifestation is known to severely impact the main meat quality traits of fast-growing chickens, such as pHu, color (L*, a*, b*), and hardness (Tasoniero et al., 2016; Baldi et al., 2018; Che et al., 2022; Barbut et al., 2024). In this regard, our results reinforced prior evidence by showing significant differences among the experimental groups (WS, WB, SM, and NB) for all the considered traits. More in detail, the evaluation of physical parameters (i.e., fillet weight, height, length, and width) evidenced that NB samples were characterized by lower values of fillet weight, height, length, and width, compared to the myopathic muscles, which is in line with other evidence reported in the literature (Zambonelli et al., 2016; Xing et al., 2020; Che et al., 2022). While no differences among WS, WB and SM fillets were found in terms of fillet length and width, WB samples were characterized by a significantly higher fillet weight and height compared to the other groups. Similarly, WB-affected fillets showed significantly higher values of pHu, L*, and compression force when compared to all the other groups (Table 1). These outcomes, other than supporting results already reported in literature (Kuttappan et al., 2017; Tasoniero et al., 2020; Wang et al., 2023b), allowed us to explore the differences in the proteome profiles in relation to the phenotypic variability of quality and morphological traits measured in normal and myopathic fillets, with a special focus on the WB myopathy. Indeed, depending on the results obtain by the study, we were able to only discuss certain differences in terms of protein co-expression patterns associated with the meat quality variability clearly characterizing breast fillets affected by the woody breast condition. More specifically, it was decided to focus our attention on protein modules identified by WGCNA that were significantly correlated with at least three of the considered phenotypic traits: i.e., the brown, turquoise, green, and black modules (Table 2). It is worth noting that, among those, the turquoise module was positively correlated with the fillet weight, fillet height, pHu, and compression force. Because all these phenotypes were characterized by significantly higher values in WB samples compared to all the other groups, the significantly positive correlations of the turquoise module with these traits have been considered useful to explore proteins involved in pathways significantly associated with the occurrence of the WB myopathy. Differently, the brown, green, and black modules were overall negatively correlated with fillet weight, height, width, compression force, and pHu. The opposite directions in terms of correlation values between these protein modules and the considered traits allowed us to explore the biological meanings of the co-expressed protein networks associated with the presence/absence of broiler myopathies, with a particular reference to the WB condition.

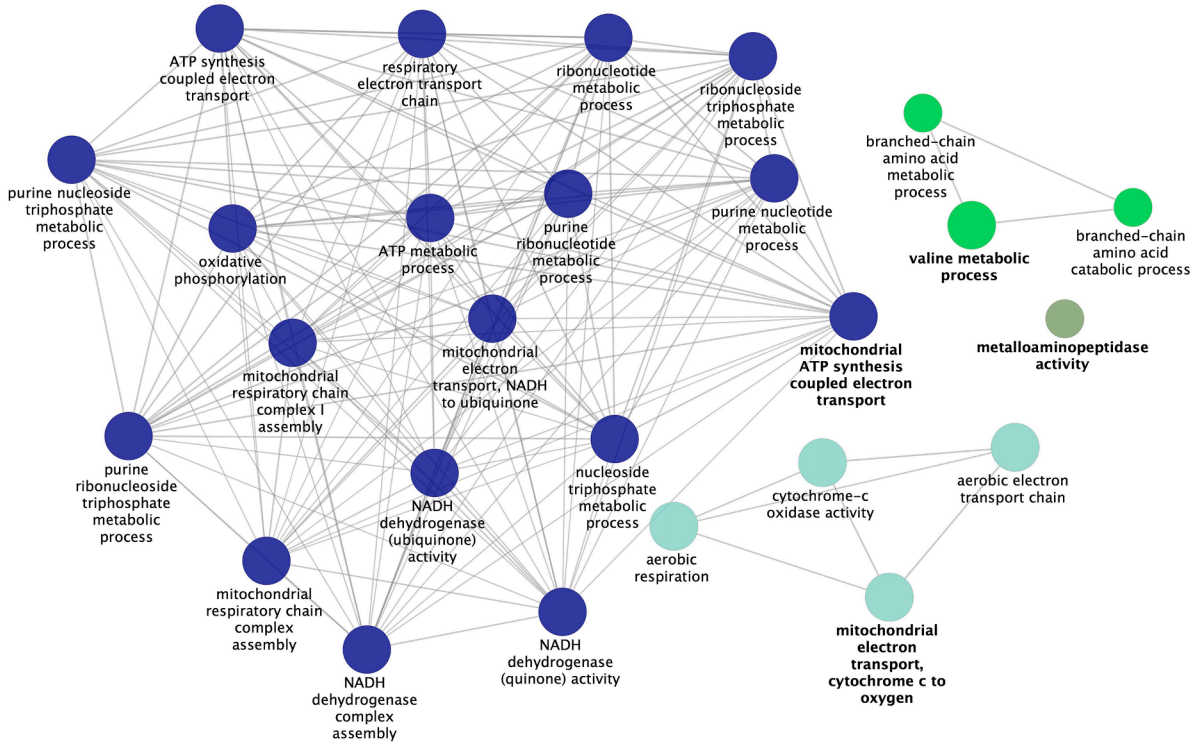

Fig. 6. ClueGO functional analysis of proteins belonging to the **black** module. The figure shows the most significant GO terms (Biological Process) identified by the ClueGO Cytoscape plugin and how terms are grouped and interact with each other. Different groups of functional terms are distinguished by different colors. Terms displaying the same color belong to the same network of functional terms, based on the *kappa* statistics score: 0.7. Terms reported in bold indicate the leading group of each GO term (according to Benjamini-Hochberg FDR adjusted *P* value), while nodes size reflects the enrichment significance of the terms: terms having the biggest node size are the most significant ones.

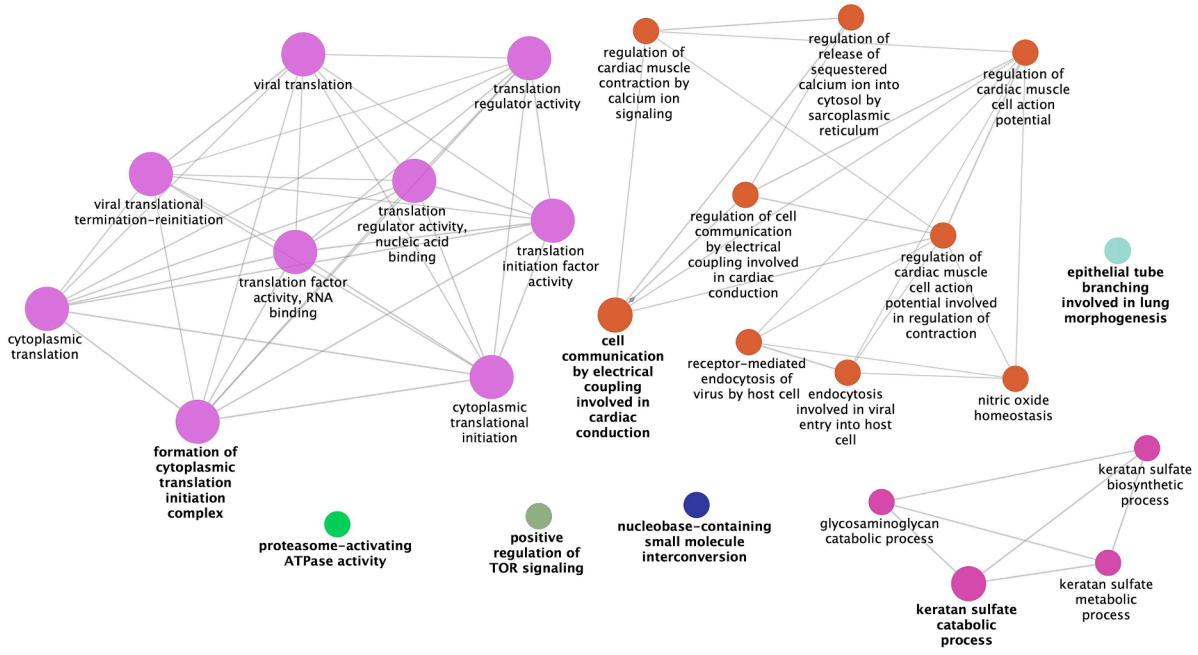

Fig. 7. ClueGO functional analysis of proteins belonging to the **green** module. The figure shows the most significant GO terms (Biological Process) identified by the ClueGO Cytoscape plugin and how terms are grouped and interact with each other. Different groups of functional terms are distinguished by different colors. Terms displaying the same color belong to the same network of functional terms, based on the *kappa* statistics score: 0.7. Terms reported in bold indicate the leading group of each GO term (according to Benjamini-Hochberg FDR adjusted *P* value), and nodes size reflects the enrichment significance of the terms: terms having the biggest node size are the most significant ones.

Besides, we performed functional enrichment analyses to point out the most relevant functional terms associated with proteins entering these selected modules to investigate more in depth the biological processes, molecular functions and cellular components involved in these

Table 3
DAVID functional annotation. Gene ontology (GO) term enrichment (BP: Biological Process; MF: Molecular Function; CC: Cellular Component) for proteins in the **turquoise** module. Benjamini-Hochberg false discovery rate (FDR) adjusted *P* value < 0.01.

Category	Term	Protein Count	Adjusted *P* value
GOTERM_BP	GO:0090148~membrane fission	18	2.39E-06
	GO:0006511~ubiquitin-dependent protein catabolic process	44	1.03E-04
	GO:2000434~regulation of protein neddylation	10	1.20E-04
	GO:0098869~cellular oxidant detoxification	21	2.81E-04
	GO:0060048~cardiac muscle contraction	15	6.62E-04
	GO:0000338~protein deneddylation	8	8.83E-04
	GO:2000767~positive regulation of cytoplasmic translation	9	1.73E-03
	GO:0006937~regulation of muscle contraction	8	2.93E-03
	GO:0051128~regulation of cellular component organization	8	2.93E-03
	GO:0045116~protein neddylation	10	2.95E-03
	GO:0006096~glycolytic process	15	2.95E-03
	GO:0034314~Arp2/3 complex-mediated actin nucleation	10	7.60E-03
	GO:0030048~actin filament-based movement	9	7.60E-03
	GO:0070934~CRD-mediated mRNA stabilization	7	7.60E-03
	GO:0035542~regulation of SNARE complex assembly	7	7.60E-03
	GO:0002183~cytoplasmic translational initiation	7	7.60E-03
	GO:0030049~muscle filament sliding	8	9.85E-03
	GO:0006164~purine nucleotide biosynthetic process	8	9.85E-03
GOTERM_MF	GO:0005523~tropomyosin binding	15	4.08E-05
	GO:0003755~peptidyl-prolyl cis-trans isomerase activity	40	6.00E-04
	GO:0140839~RNA polymerase II CTD heptapeptide repeat P3 activity	42	1.02E-03
	GO:0140840~RNA polymerase II CTD heptapeptide repeat P6 activity	42	1.02E-03
	GO:0000146~microfilament motor activity	38	1.55E-03
	GO:0160072~ubiquitin ligase complex scaffold activity	8	6.40E-03
GOTERM_CC	GO:0005865~striated muscle thin filament	9	9.38E-06
	GO:0032982~myosin filament	11	3.22E-05
	GO:0005885~Arp2/3 protein complex	8	6.20E-05
	GO:0008180~COP9 signalosome	13	9.15E-05
	GO:0000145~exocyst	9	1.21E-04
	GO:0031588~nucleotide-activated protein kinase complex	8	1.21E-04
	GO:0030665~clathrin-coated vesicle membrane	12	2.51E-04
	GO:0000502~proteasome complex	16	3.21E-04
	GO:0031461~cullin-RING ubiquitin ligase complex	8	6.21E-04
	GO:0012506~vesicle membrane	12	9.44E-04
	GO:0030127~COPII vesicle coat	8	9.78E-04
	GO:0070971~endoplasmic reticulum exit site	11	1.19E-03
	GO:0005643~nuclear pore	20	1.33E-03
	GO:0005851~eukaryotic translation initiation factor 2B complex	5	1.48E-03
	GO:0016459~myosin complex	13	3.07E-03
	GO:0016460~myosin II complex	9	3.12E-03
	GO:0030131~clathrin adaptor complex	6	3.80E-03
	GO:0030016~myofibril	10	8.93E-03

Table 4
DAVID functional annotation. Gene ontology (GO) term enrichment (GOTERM_BP: Biological Process; GOTERM_MF: Molecular Function; GOTERM_CC: Cellular Component) for proteins in the **brown** module. Benjamini-Hochberg false discovery rate (FDR) adjusted *P* value < 0.01.

Category	Term	Protein Count	Adjusted *P* value
GOTERM_BP	GO:0007007~inner mitochondrial membrane organization	8	9.63E-08
	GO:0006122~mitochondrial electron transport, ubiquinol to cytochrome c	7	3.17E-07
	GO:0042407~cristae formation	7	6.25E-07
	GO:0045333~cellular respiration	8	9.62E-06
	GO:0006086~acetyl-CoA biosynthetic process from pyruvate	5	2.83E-05
GOTERM_MF	GO:0034604~pyruvate dehydrogenase (NAD+) activity	5	3.15E-05
	GO:0009055~electron transfer activity	7	2.51E-03
	GO:0015078~proton transmembrane transporter activity	5	8.02E-03
GOTERM_CC	GO:0045275~respiratory chain complex III	7	2.30E-08
	GO:0140275~MIB complex	6	1.46E-06
	GO:0001401~SAM complex	6	1.46E-06
	GO:0045254~pyruvate dehydrogenase complex	5	8.86E-06
	GO:0005788~endoplasmic reticulum lumen	13	2.55E-04
	GO:0062023~collagen-containing extracellular matrix	14	4.07E-04
	GO:0005604~basement membrane	7	2.61E-03
	GO:0045273~respiratory chain complex II (succinate dehydrogenase)	3	5.68E-03

Table 5
DAVID functional annotation. Gene ontology (GO) term enrichment (GOTERM_BP: Biological Process; GOTERM_MF: Molecular Function; GOTERM_CC: Cellular Component) for proteins in the **black** module. FDR adjusted *P* value < 0.01.

Category	Term	Protein Count	Adjusted *P* value
GOTERM_BP	GO:0009060~aerobic respiration	32	6.63E-61
	GO:0006120~mitochondrial electron transport, NADH to ubiquinone	29	1.09E-59
	GO:0042776~proton motive force-driven mitochondrial ATP synthesis	31	1.09E-59
	GO:0032981~mitochondrial respiratory chain complex I assembly	27	2.39E-48
	GO:1902600~proton transmembrane transport	31	1.39E-44
	GO:0045333~cellular respiration	8	1.10E-09
	GO:0006123~mitochondrial electron transport, cytochrome c to oxygen	7	2.11E-09
GOTERM_MF	GO:0008137~NADH dehydrogenase (ubiquinone) activity	30	7.97E-64
	GO:0004129~cytochrome-c oxidase activity	4	3.09E-04
GOTERM_CC	GO:0045271~respiratory chain complex I	31	3.46E-66
	GO:0005743~mitochondrial inner membrane	40	1.60E-46
	GO:0005739~mitochondrion	45	4.41E-33
	GO:0045277~respiratory chain complex IV	7	1.19E-09

myopathies. Functional annotations of proteins entering the considered co-expressed networks are discussed below.

Turquoise module

Functional analysis of proteins enriching the turquoise module – positively correlated with fillet weight, height, pHu, and compression

Table 6
DAVID functional annotation. Gene ontology (GO) term enrichment (GOTERM_BP: Biological Process; GOTERM_MF: Molecular Function; GOTERM_CC: Cellular Component) for proteins in the **green** module. Benjamini-Hochberg false discovery rate (FDR) adjusted *P* value < 0.01.

Category	Term	Protein Count	Adjusted *P* value
GOTERM_BP	GO:0001732~formation of cytoplasmic translation initiation complex	7	9.21E-08
	GO:0006413~translational initiation	8	4.13E-06
	GO:0075525~viral translational termination-reinitiation	4	3.52E-04
GOTERM_MF	GO:0003743~translation initiation factor activity	8	3.43E-06
	GO:0030021~extracellular matrix structural constituent conferring compression resistance	4	4.08E-03
GOTERM_CC	GO:0005852~eukaryotic translation initiation factor 3 complex	7	1.53E-08
	GO:0033290~eukaryotic 48S preinitiation complex	7	1.53E-08
	GO:0016282~eukaryotic 43S preinitiation complex	7	1.67E-08
	GO:0071541~eukaryotic translation initiation factor 3 complex, eIF3m	4	1.46E-04

Table 7
Abundance of target proteins (COL3A1, COL4A1, and COL4A2) in wooden breast (WB) samples expressed as fold change relative to the control group (NB). Differences in the normalized abundance of each target protein between WB and NB were assessed by Mann-Whitney U-test.

Target protein	Symbol	Molecular weight (kDa)	Fold Change	*P* value
Collagen type III alpha 1 chain	COL3A1	114	1.51	0.08
Collagen type IV alpha 1 chain	COL4A1	119	1.04	0.66
Collagen type IV alpha 2 chain	COL4A2	116	0.52	0.08

force – evidenced several terms already reported to be associated with the WB occurrence and progression. Among those, "cellular oxidant detoxification" and "antioxidant activity" identified respectively by the DAVID tool and ClueGO functional analyses are in line with the cellular mechanisms that may occur as a response to the oxidative stress condition characterizing WB-affected muscles (Mutryn et al., 2015; Petracci et al., 2019; Xing et al., 2021; Barbut et al., 2024; Wang et al., 2025). More in detail, proteins enriching these functional terms belong to the Glutathione S-transferases (**GSTs**) family (e.g., Glutathione S-transferase kappa, GSTK1; Glutathione S-transferase Mu 2, GSTM2; Glutathione S-transferase omega 2; GSTO2; Glutathione S-transferase theta-1, GSTT1), which play significant roles in antioxidant protective response, especially through reactive oxygen species (**ROS**) detoxification (Alnasser, 2025). Notably, in humans, the GSTM2 involvement in attenuating DNA damage in cardiomyocytes under cardiac hypertrophy conditions has been demonstrated (Xu et al., 2023). This could be considered in line with the DNA damage response during oxidative stress events hypothesized to occur in samples affected by both WB and WS myopathies (Bordini et al., 2022). Also, several peroxiredoxins – a family of cysteine (Cys)-centered redox proteins exerting multiple roles in redox-reactive reactions in physiological and pathological processes (Stancill and Corbett, 2022) – were found enriching the "cellular oxidant detoxification" term: Peroxiredoxin-3 (PRDX3), Peroxiredoxin-4 (PRDX4), and Peroxiredoxin-6 (PRDX6). These proteins are actively involved in protecting cells from oxidative damage by reacting with hydrogen peroxide, peroxynitrite, or lipid peroxides (Stancill and Corbett, 2022). Different peroxiredoxin isoforms differ in their subcellular localization. Specifically, PRDX3 localizes into mitochondria, while PRDX4 and PRDX6 localize to the endoplasmic reticulum and cytoplasm, respectively (Stancill and Corbett, 2022), thus suggesting disseminating oxidative stress events taking place in different cellular compartments. As additional players involved in antioxidant activity, Glutathione Peroxidase 1 (GPX1) and Glutathione Peroxidase 3 (GPX3) were found in our study. In accordance with our results, Carvalho et al. (2023) evidenced through label-free comparative proteomic analysis an increased abundance of PRDX1, PRDX6, and Glutathione S-transferase (GSH-ST) in WB samples. Researchers hypothesized the involvement of these proteins in contrasting the pro-oxidative status occurring in affected samples (Carvalho et al., 2023; Petracci et al., 2019). However, as recently reviewed by Wang et al. (2025), the excessive production of ROS taking place in WB muscles overcome the muscle ability of the tissue to implement efficient antioxidant defense, thus resulting in an inefficient cellular response to detoxification.

As for other terms consistent with the results reported by Carvalho et al. (2023), "Arp2/3 complex-mediated actin nucleation" and "Arp2/3 protein complex" were identified in the present study. In this regard, Carvalho et al. (2023) found an increased abundance of Arp2/3 complex 34 kDa subunit in muscles affected by WB and hypothesized its involvement in the functional alterations of myofibrillar proteins and cross-linking of actin filaments, possibly contributing to the higher hardness observed in WB meat. In our study, Arp2/3 complex subunit 2 and 3 (ARPC2 and ARPC3), Actin-related protein 3 (ACTR3), and Actin-related protein 2 (ACTR2) were among the proteins entering these functional terms and, thus, the network of co-expressed proteins positively associated with the compression force trait. These proteins are known to be involved in the actin polymerization process, which consists of constructing new actin filament networks by promoting actin nucleation for the formation of a new branch from an existing filament and play pivotal roles in myoblast fusion, which is crucial for a proper muscle development (Pollard and Beltzner, 2002; Bai et al., 2023). These results seemed to support evidence of their involvement in the higher hardness observed in WB meat. Also, it could be speculated that an altered activity of the Arp2/3 complex may be associated with the degeneration/regeneration processes undergoing the breast muscles affected by WB myopathy.

Breast muscles affected by the growth-related myopathies, with special reference to WB, have been reported to exhibit an altered sarcomere architecture (Velleman and Clark, 2015; Papah et al., 2017; Velleman et al., 2017; Liu et al., 2020). In this regard, the present study evidenced several proteins composing sarcomeric structures, such as Tropomodulin subunits (i.e., TMD1, TMOD3, and TMOD4) and numerous Myosin heavy chain isoforms (MYH7, MYH9, MYH10, MYH11, and MYH15) as part of the turquoise module and enriched in the following functional terms: "myosin filament", "myofibril", "tropomyosin binding", and "striated muscle thin filament". These results strengthened the evidence of alterations at the sarcomere level in myopathic muscles.

Interestingly, some of the sarcomeric proteins enriched in these terms are reported in the literature as specific isoforms of cardiac muscles. For instance, three different Myosin Binding Protein-C (MyBP-C) were identified in the turquoise module: two expressed in skeletal muscle (MYBPC1 and MYBPC2) and one predominantly expressed in cardiac muscle (MYBPC3) (McNamara and Sadayappan, 2018). Several studies reported that, in humans, the expression of the cardiac-type isoform is restricted to cardiac muscles and that mutations in its coding gene are causative of different cardiomyopathies (e.g., hypertrophic cardiomyopathy and dilated cardiomyopathy) (Lin et al., 2013; McNamara and Sadayappan, 2018; Song et al., 2023). Otherwise, in chickens, the cardiac-type isoform of Myosin Binding Protein-C has been detected not only in cardiac muscles, but also as transiently expressed at the early stage of skeletal muscle development, before skeletal muscle-type isoforms become detectable (Yasuda et al., 1995). In this regard, it could be speculated that an abnormal expression of the cardiac-type isoform in adult skeletal muscles might be related to a shift toward an

embryonic-like expression pattern in myopathic fillets. This would be in line with the theory reported by Velleman (2020) that took into consideration the higher expression level of specific components of the extracellular matrix of WB muscles (e.g., Collagen type III), which are known to be highly expressed during the early stage of muscle development. However, it could also be speculated that the activation of embryonic molecular pathways may be ascribable to the regeneration processes taking place in myopathic muscles. A different hypothesis has been suggested by Padilha et al. (2024), who investigated candidate genes potentially involved in WS condition through RNA-sequencing. The results published by this study evidenced genes encoding for the MYBPC1 and MYBPC3 isoforms as upregulated in WS-affected muscles, leading the researchers to conclude that the upregulation of these genes might be involved in the shift from fast- to slow-muscle fiber's development, thus altering muscle structure and affecting the functional properties of the skeletal muscle (Padilha et al., 2024).

It is also worth noting that, in humans, MYBPC3 is associated with the development of hypertrophic cardiomyopathy. This is particularly interesting when considering that, in our study, the ClueGO analysis evidenced several functional terms related to cardiac muscle development and organization, such as "cardiac muscle fiber development", "cardiac myofibril assembly", and "cardiac muscle cell differentiation". Similarly, "cardiac muscle contraction" was found to be a significant term for the turquoise module by DAVID tool. Proteins enriching these terms (e.g., TNNT2 and CSRP3), some of those already mentioned in this discussion (e.g., MYH7 and MYBPC3), belong to common genetic pathways in cardiomyopathies among different species, humans, cattle, turkeys, chickens, and companion animals (Simpson et al., 2017). Therefore, it could be hypothesized as an association between the WB condition and biological pathways involved in cardiac myopathy. Similarly, Che et al. (2023) suggested that WB may predispose broiler to dorsal recumbency syndrome, which leads birds to death due to cardio-pulmonary insufficiency. However, a recent study investigating cardiac implications of chicken WB myopathy (Støle et al., 2025) showed no signs of fibrosis in hearts of chickens affected by this condition, even though the study did not take into consideration hearts of birds showing no signs of myopathy at the skeletal muscle level. In this regard, the authors highlighted the lack of a healthy control group as a limitation of the study. Nevertheless, at the transcriptomic level, the study evidenced differences between muscles showing various degrees of WB and concluded that they may become more prominent with age, potentially leading to cardiac dysfunction (Støle et al., 2025).

Different fibrillar collagen proteins were also found entering the turquoise module: Collagen type III alpha 1 chain (COL3A1), Collagen type V alpha 1 chain (COL5A1), Collagen type I alpha 1 chain (COL1A1), and Collagen type VI alpha 3 chain (COL6A3). These specific types of fibrillar collagen – representing some of the major players of the extracellular matrix (**ECM**) of muscular and connective tissues – are known to exert crucial roles in the proper development and maintenance of skeletal muscle structure and function, both in mammals and birds (Velleman, 2002; Csapo et al., 2020; Zhang et al., 2021). The positive correlation values between the co-expression network they belonged to and the phenotypic variability of fillet weight, height, pHu and compression force are in line with the higher expression level found for these proteins and their coding genes in myopathic muscles, already reported in the literature. In particular, numerous scientific studies identified genes coding for alpha chains composing the Collagen type I, III, and VI proteins as upregulated in breast muscles affected by WB myopathy (Pampouille et al., 2018; Papah et al., 2018; Praud et al., 2020; Zhang et al., 2024; Zhao et al., 2024). Notably, COL6A3 coding gene has been found as a hub gene in a previous WGCNA study considering microarray data to identify molecular pathways and key genes involved in WS and WB occurrences (Bordini et al., 2022). Similarly, in the same study, the gene coding for the alpha 2 chain of Collagen type V (COL5A2) was one of the hub genes detected by the analysis. A recent study by Zhang et al. (2024), performing a meta-analysis using 5 different transcriptomic datasets to identify differentially expressed and hub genes associated with WB myopathy, detected *COL1A1, COL1A2, COL3A1, COL6A2*, and*COL6A3* genes as hub nodes in the molecular pathways associated with this myopathy. In line with this, the results obtained in the present study by western blot analysis, showing a tendency of a 1.51-fold higher expression of COL3A1 in WB compared to the normal ones, corroborate the assumption of its involvement in this condition, which has been suggested by the positive correlation between the turquoise module and the phenotypic variability of fillet weight and height as well as pHu, and compression force.

Furthermore, types of collagens belonging to the FACIT (Fibril-Associated Collagens with Interrupted Triple helices) family (Kaur and Reinhardt, 2015) were also found in the turquoise module: the Collagen type XIV alpha 1 chain (COL14A1) and Collagen type XII alpha 1 chain (COL12A1). As for these two collagen proteins, Che et al. (2024) showed higher expression levels of the second one coding gene (*COL12A1*) in WB samples compared to the normal breast, while no significant differences in the *COL14A1* transcription level were found. On the contrary, Papah et al. (2018) reported a higher expression level of *COL14A1* in WB-affected compared to non-affected samples, which is in accordance with the results obtained in this study.

Overall, the higher expression both at the gene and protein levels of these components is in line with the extensive fibrosis characterizing WB muscles. Indeed, an aberrant deposition of ECM components has been hypothesized to be one of the key events leading to the impressive fibrosis commonly observed in WB (Velleman, 2020, 2023). Considering all the above, our results corroborate the evidence of a strong positive relationship between the occurrence of the WB myopathy and the exceptional deposition of fibrillar collagen proteins.

Brown module

The protein co-expression network identified by WGCNA as the brown module, showing a negative correlation with fillet weight, width, and height traits, was also investigated. Because of its negative correlation with these traits, a negative correlation with WB myopathy can be speculated. It is worth noting, especially if considering the results discussed above for the turquoise module, that several non-fibrillar collagen proteins composing the basement membrane of skeletal muscle tissues were found in this module. More specifically, within the "basement membrane" category referring to cellular component functional terms, the non-fibrillar Collagen types XV and XVIII were found (i.e., COL15A1 and COL18A1). Although non-fibrillar collagens remain relatively less characterized compared to the fibrillar ones, they are increasingly recognized for their diverse roles in physiological and pathological processes, including tissue growth, homeostasis, repair, and disease (Bretaud et al., 2020). Type XV collagen is part of an evolutionarily conserved subgroup of non-fibrillar basement membrane (BM)-associated collagens known as multiplexins, which are defined by their multiple interrupted triple-helical domains (Bretaud et al., 2020). This subgroup also includes the structurally related Collagen type XVIII (Bretaud et al., 2020). Interestingly, Collagen type XV has been reported to function as a crucial structural component stabilizing skeletal muscle cells and microvessels in humans and mice (Eklund et al., 2001; Muona et al., 2002). Besides, the study by Eklund et al. (2001) performed histological analysis of skeletal muscle from *COL15A1-null* mice and revealed features consistent with myopathic disorders, including degenerating fibers, an increased proportion of centrally nucleated myofibers, and fiber size variability. These alterations emerged by approximately 3 months of age and became more pronounced with advancing age (Eklund et al., 2001). The pronounced alterations observed in Collagen type XV-deficient muscle fibers likely reflect a disruption in the linkage between the muscle cell basement membrane and the surrounding fibrillar ECM. Thus, in WB-affected birds, the lower abundance of the non-fibrillar Collagen type XV could be involved in the insufficient stabilization of muscle cells. Additional non-fibrillar

collagen proteins entering the brown module are the two alpha chains composing Collagen type IV: Collagen type IV alpha 1 (COL4A1) and Collagen type IV alpha 2 (COL4A2). Intriguingly, the present results suggested a lower expression of non-fibrillar collagens composing the basement membrane of the skeletal muscles of WB-affected birds, which is in line with the 0.52-fold change expression ($P = 0.08$) of COL4A2 in WB compared to NB evidenced by the western blot analysis. Thus, considering the essential roles played by these collagens in maintaining the integrity of the ECM (Csapo et al., 2020), their involvement in the alterations characterizing WB muscles could be speculated (Velleman, 2020). In this regard, our previous research paved the way for hypothesizing the involvement of alterations of Collagen type IV as a factor potentially contributing to activating the endoplasmic reticulum stress either at the muscular or vascular level, which is supposed to be one of the primary alterations characterizing muscles affected by growth-related myopathies (Bordini et al., 2021, 2022, 2024).

Moreover, functional enrichment analyses performed using both the DAVID tool and ClueGO pointed out several terms related to the mitochondrial inner membrane organization and function, specifically referring to structural aspects (e.g., "inner membrane organization" and "cristae formation"), molecular machinery (e.g., "respiratory chain complex III"), and metabolic processes (e.g., "mitochondrial electron transport" and "oxidative phosphorylation"). Among the proteins enriching these terms, several Ubiquinol-Cytochrome c Reductase subunits (UQCRQ, UQCRC1, UQCRC2, UQCR10, and UQCR11) composing the respiratory chain complex III, as well as Ubiquinol-Cytochrome c Reductase Binding Protein (UQCRB), were found. Besides, proteins involved in the tricarboxylic acid (**TCA**) cycle were found enriching the "Pyruvate dehydrogenase (NAD+) activity" and "acetyl-CoA biosynthetic process from pyruvate" functional terms. More specifically, the Pyruvate dehydrogenase complex subunits (e.g., PDHX, PDHB and PDHA2) were some of the proteins found in the brown module. Similar results showing a significant downregulation of PDHB and PDHX coding genes in WB samples were reported by Zhang et al. (2024). Overall, these results agreed with the theory of a downgraded TCA cycle and dysregulated mitochondrial functionality supported by the evidence reported in several studies (Papah et al., 2017; Hosotani et al., 2020; Lake et al., 2021; Wang et al., 2023a; Bordini et al., 2024).

Black module

Similar to what has been found for the brown module, proteins belonging to the black module were significantly enriched with functional terms related to mitochondrial activity (e.g., "respiratory chain complex I", "mitochondrial electron transport, NADH to ubiquinone", and "aerobic respiration"). Considering the negative correlation between the black module and fillet weight, length, height, compression force, and pHu, these results further strengthened the evidence of dysregulated mitochondrial activity in WB samples compared to the normal ones, with a specific reference to some of the complexes involved in the oxidative phosphorylation. Indeed, subunits of the complex I of the respiratory chain, such as NADH-ubiquinone oxidoreductase chains (MT-ND6, MT-ND1, and MT-ND4) and several NADH dehydrogenase subunits (e.g., NDUFA5, NDUFA2, NDUFC2, NDUFS8, NDUFS7, NDUFS6, NDUFS5, and NDUFAB1) were among the proteins entering the brown co-expression network. Lower expression levels of genes encoding several subunits of the complex I in WB chickens were described by previous studies (Papah et al., 2017; Hosotani et al., 2020; Hasegawa et al., 2022; Wang et al., 2023a; Bordini et al., 2024). Most recently, Greene et al. (2025b) demonstrated altered mitochondrial biogenesis, morphology and activity in WB by showing downregulation in gene/protein expression of players involved in OXPHOS and ATP production. Because complex I dysfunction is one of the most common OXPHOS alterations, and abnormalities in the complex I assembly process are often associated with mitochondrial abnormalities (Mimaki et al., 2012), the present results support the overall altered mitochondria biogenesis and functionality described in WB-affected tissues (Lake et al., 2021; Bordini et al., 2024; Greene et al., 2025b).

Green module

Functional enrichment analyses performed by both the DAVID tool and ClueGO evidenced the "formation of the cytoplasmic translational complex" as well as other related terms such as the "eukaryotic translation initiation factor 3 complex", representing a crucial step in protein synthesis (Hinnebusch, 2006; Jackson et al., 2010), as significant categories enriching the proteins belonging to the green module. In the process of protein synthesis, translation initiation is considered a rate-limiting step and is controlled by the availability and activity of the eIFs protein family, among which eIF3 is one of the most intricate members (Hinnebusch, 2006; Wolf et al., 2020). Our results showed several eIF3 complex subunits (EIF3K, EIF3L, EIF3I, EIF3G, EIF3H, EIF3D, and EIF3A) belonging to the green module. In broiler chickens, a comparative study using proteomics to investigate the effects of creatine pyruvate on lipid and protein metabolism (Chen et al., 2012) showed a higher expression of eukaryotic translation initiation factors 2 and 3. Due to their role in initiating the protein synthesis process, the researchers concluded that their greater expression in the experimental group (supplemented with 5% creatine pyruvate) may have resulted in increased protein synthesis and cell growth (Chen et al., 2012). In our study, the negative correlation between the green module and the traits showing significantly higher values in WB compared to NB let us assume a reduction in the eIF3 Complex presence and activity in myopathic muscles. Notably, in humans and animal models, the loss/depletion of eIF3 is associated with decreased synthesis of mitochondrial proteins and decreased Complex I activity in skeletal muscle (Wolf et al., 2020), which overlap the results highlighted in the present study as well as those previously reported in the literature (Papah et al., 2017; Hosotani et al., 2020; Wang et al., 2023a). Furthermore, taking into consideration the relevant role of the eIF3 complex in the protein synthesis process, it could be noted that these proteins were found as negatively correlated with those traits significantly characterizing WB muscles. This could be considered slightly unexpected since, as reviewed by Soglia et al. (2021), the outstanding breast muscle development achieved by fast-growing broilers certainly requires an increased protein deposition. However, Soglia et al. (2021) also reported that this intensification in protein synthesis could potentially overcome the capability of some cellular structures involved in this process (e.g., endoplasmic reticulum) and fail to properly monitor and optimize protein folding, thus leading to the buildup and accumulation of deleterious misfolded or dysfunctional proteins. Thus, in view of the role of the eIF3 complex in recruiting protein quality-control factors (Sha et al., 2009; Wolf et al., 2020), alteration of this process due to a depletion in their expression and activity could also be speculated.

Conclusions

Overall, the present study applied for the first time a co-expression network analysis to proteomic data, aiming at further exploring the biological mechanisms and cellular components potentially involved in the occurrence of the breast myopathies affecting fast-growing chickens. In view of the differences found between WS, WB, SM and the not-affected fillets in terms of meat quality evaluation, results gained by the WGNCA analysis performed combining the proteomic profiles and meat quality data of chicken fillets affected by myopathies allowed us to consider this approach suitable for exploring protein expression networks involved in the occurrence of these myopathies, with a particular reference to the WB condition due to the specific results gained in the present study. To strengthen this assumption, it could be noted that the results obtained in this study were largely in accordance with a wealth of literature regarding transcriptomic and proteomic characterizations of breast muscles affected by these myopathies. In this sense, the outcomes

of the present study provided further evidence for the involvement of extracellular matrix and mitochondrial dysfunctions in WB. As novel outcomes, different roles between fibrillar (e.g., COL1A1, COL3A1, COL5A1, and COL6A3) and non-fibrillar collagens (COL4A1, COL4A2, COL15A1, and COL18A1) in the characterization of this condition have been hypothesized. Furthermore, impairment of the molecular processes involved in protein synthesis and quality-control, mainly regarding the eIF3 complex, thus potentially leading to the accumulation of aberrant proteins in WB tissues, could be speculated. Considering the somewhat small sample dataset used for this work, additional research involving a larger sample size is recommended to broaden the considerations and assumptions raised in this study. Also, to expand this approach to find patterns of co-expressed proteins specifically characterizing the WS and SM defects, further studies should include additional traits clearly distinguishing these conditions and thus allowing a more focused investigation of protein expression patterns associated with these specific myopathies affecting fast-growing chickens.

CRediT authorship contribution statement

Martina Bordini: Writing – original draft, Methodology, Investigation, Formal analysis, Data curation, Conceptualization. **Massimiliano Petracci:** Writing – original draft, Validation, Supervision, Investigation. **Francesca Soglia:** Writing – review & editing, Validation, Supervision, Investigation, Conceptualization. **Shai Barbut:** Writing – review & editing, Validation, Supervision, Resources, Project administration, Investigation, Data curation, Conceptualization.

Disclosures

The authors declare that they have no known competing financial interests or personal relationships that could have appeared to influence the work reported in this paper.

Acknowledgments

The authors would like to thank Chaoyue Wang and Weilun Lin (Department of Food Science, University of Guelph, Ontario, Canada) for help processing some of the fresh meat. The research has been partially funded by NextGenerationEU, National Grant PRIN2022 (Prot. n. 2022EPWEPW).

Supplementary materials

Supplementary material associated with this article can be found, in the online version, at doi:10.1016/j.psj.2026.106818.

References

Alnahhas, N., Pouliot, E., Saucier, L., 2023. The hypoxia-inducible factor 1 pathway plays a critical role in the development of breast muscle myopathies in broiler chickens: a comprehensive review. Front. Physiol. 14, 1260987.
Alnasser, S.M., 2025. The role of glutathione S-transferases in human disease pathogenesis and their current inhibitors. Genes. Dis. 12, 101482.
Bai, Y., Zhao, F., Wu, T., Chen, F., Pang, X., 2023. Actin polymerization and depolymerization in developing vertebrates. Front. Physiol. 14, 1213668.
Bailey, R.A., Watson, K..A., Bilgili, S.F., Avendano, S., 2015. The genetic basis of pectoralis major myopathies in modern broiler chicken lines. Poult. Sci. 94, 2870–2879.
Bailey, R.A., Souza, E.., Avendano, S., 2020. Characterising the influence of genetics on breast muscle myopathies in broiler chickens. Front. Physiol. 11, 1041.
Bailey, R.A., 2023. Strategies and opportunities to control breast myopathies: an opinion paper. Front. Physiol. 14, 1173564.
Baldi, G., Soglia, F., Mazzoni, M., Sirri, F., Canonico, L., Babini, E., Laghi, L., Cavani, C., Petracci, M., 2018. Implications of white striping and spaghetti meat abnormalities on meat quality and histological features in broilers. Animal. 12, 164–173.
Barbut, S., Mitchell, R., Hall, P., Bacon, C., Bailey, R., Owens, C.M., Petracci, M., 2024. Review: myopathies in broilers: supply chain approach to provide solutions to challenges related to raising fast growing birds. Poult. Sci. 103, 103801.
Bateman, A., Martin, M.J., Orchard, S., Magrane, M., Adesina, A., Ahmad, S., Bowler-Barnett, E.H., Bye-A-Jee, H., Carpentier, D., Denny, P., Fan, J., Garmiri, P., da Costa Gonzales, L.J., Hussein, A., Ignatchenko, A., Insana, G., Ishtiaq, R., Joshi, V., Jyothi, D., Kandasaamy, S., Lock, A., Luciani, A., Luo, J., Lussi, Y., Marin, J.S.M., Raposo, P., Rice, D.L., Santos, R., Speretta, E., Stephenson, J., Totoo, P., Tyagi, N., Urakova, N., Vasudev, P., Warner, K., Wijerathne, S., Yu, C.W.H., Zaru, R., Bridge, A. J., Aimo, L., Argoud-Puy, G., Auchincloss, A.H., Axelsen, K.B., Bansal, P., Baratin, D., Batista Neto, T.M., Blatter, M.C., Bolleman, J.T., Boutet, E., Breuza, L., Gil, B.C., Casals-Casas, C., Echioukh, K.C., Coudert, E., Cuche, B., de Castro, E., Estreicher, A., Famiglietti, M.L., Feuermann, M., Gasteiger, E., Gaudet, P., Gehant, S., Gerritsen, V., Gos, A., Gruaz, N., Hulo, C., Hyka-Nouspikel, N., Jungo, F., Kerhornou, A., Le Mercier, P., Lieberherr, D., Masson, P., Morgat, A., Paesano, S., Pedruzzi, I., Pilbout, S., Pourcel, L., Poux, S., Pozzato, M., Pruess, M., Redaschi, N., Rivoire, C., Sigrist, C.J.A., Sonesson, K., Sundaram, S., Sveshnikova, A., Wu, C.H., Arighi, C.N., Chen, C., Chen, Y., Huang, H., Laiho, K., Lehvaslaiho, M., McGarvey, P., Natale, D.A., Ross, K., Vinayaka, C.R., Wang, Y., Zhang, J., 2025. UniProt: the Universal protein knowledgebase in 2025. Nucleic. Acids. Res. 53, D609–D617.
Bindea, G., Mlecnik, B., Hackl, H., Charoentong, P., Tosolini, M., Kirilovsky, A., Fridman, W.H., Pagès, F., Trajanoski, Z., Galon, J., 2009. ClueGO: a Cytoscape plug-in to decipher functionally grouped gene ontology and pathway annotation networks. Bioinformatics. 25, 1091–1093.
Bordignon, F., Xiccato, G., Boskovic Cabrol, M., Birolo, M., Trocino, A., 2022. Factors affecting breast myopathies in broiler chickens and quality of defective meat: a meta-analysis. Front. Physiol. 13, 933235.
Bordini, M., Zappaterra, M., Soglia, F., Petracci, M., Davoli, R., 2021. Weighted gene co-expression network analysis identifies molecular pathways and hub genes involved in broiler white striping and wooden Breast myopathies. Sci. Rep. 11, 1776.
Bordini, M., Soglia, F., Davoli, R., Zappaterra, M., Petracci, M., Meluzzi, A., 2022. Molecular pathways and key genes associated with breast width and protein content in white striping and wooden breast chicken pectoral muscle. Front. Physiol. 13, 936768.
Bordini, M., Wang, Z., Soglia, F., Petracci, M., Schmidt, C.J., Abasht, B., 2024. RNA-sequencing revisited data shed new light on wooden breast myopathy. Poult. Sci. 103, 103902.
Bretaud, S., Guillon, E., Karppinen, S.M., Pihlajaniemi, T., Ruggiero, F., 2020. Collagen XV, a multifaceted multiplexin present across tissues and species. Matrix. Biol. Plus. 6–7, 100023.
Carvalho, L.M., Rocha, T..C., Delgado, J., Díaz-Velasco, S., Madruga, M.S., Estévez, M., 2023. Deciphering the underlying mechanisms of the oxidative perturbations and impaired meat quality in wooden breast myopathy by label-free quantitative MS-based proteomics. Food Chem. 423, 136314.
Che, S., Wang, C., Varga, C., Barbut, S., Susta, L., 2022. Prevalence of breast muscle myopathies (spaghetti meat, woody breast, white striping) and associated risk factors in broiler chickens from Ontario Canada. PLoS. One 17, e0267019.
Che, S., Weber, L., Novy, A., Barbut, S., Susta, L., 2023. Characterization of dorsal recumbency syndrome associated with woody breast in broiler flocks from Ontario. Canada. Poult. Sci. 102, 102307.
Che, S., Pham, P.H., Barbut, S., Bienzle, D., Susta, L., 2024. Transcriptomic profiles of pectoralis major muscles affected by spaghetti meat and woody breast in broiler chickens. Animals 14, 176.
Chen, J., Huang, J., Deng, J., Ma, H., Zou, S., 2012. Use of comparative proteomics to identify the effects of creatine pyruvate on lipid and protein metabolism in broiler chickens. Vet. J. 193, 514–521.
Chen, Q., Tan, Y., Zhang, C., Zhang, Z., Pan, S., An, W., Xu, H., 2021. A weighted gene co-expression network analysis–derived prognostic model for predicting prognosis and immune infiltration in gastric cancer. Front. Oncol. 11, 221.
Csapo, R., Gumpenberger, M., Wessner, B., 2020. Skeletal muscle extracellular matrix – what do we know about its composition, regulation, and physiological roles? A narrative review. Front. Physiol. 11, 517800.
Dang, D.S., Zhai, C.., Nair, M.N., Thornton, K.J., Sawalhah, M.N., Matarneh, S.K., 2022. Tandem mass tag labeling to assess proteome differences between intermediate and very tender beef steaks. J. Anim. Sci. 100, skac042.
Du, Y., Wang, Y., Xu, Q., Zhu, J., Lin, Y., 2021. TMT-based quantitative proteomics analysis reveals the key proteins related with the differentiation process of goat intramuscular adipocytes. BMC. Genomics. 22, 417.
Eklund, L., Piuhola, J., Komulainen, J., Sormunen, R., Ongvarrasopone, C., Fässler, R., Muona, A., Ilves, M., Ruskoaho, H., Takala, T.E.S., Pihlajaniemi, T., 2001. Lack of type XV collagen causes a skeletal myopathy and cardiovascular defects in mice. Proc. Natl. Acad. Sci. USA 98, 1194–1199.
Greene, E.S., Che, S.., Soglia, F., Iwasaki, T., Watanabe, T., Kawasaki, T., Susta, L., Petracci, M., Scanes, C., Dridi, S., 2025a. Breast muscle myopathies: twists and turns in modern broilers. Avian Pathol. 54, 669–692.
Greene, E.S., Chen, P..R., Walk, C., Bedford, M., Dridi, S., 2025b. Mitochondrial dysfunction is a hallmark of woody breast myopathy in broiler chickens. Front. Physiol. 16, 1543788.
Hasegawa, Y., Hosotani, M., Saito, M., Nagasawa, T., Mori, Y., Kawasaki, T., Yamada, M., Maeda, N., Watanabe, T., Iwasaki, T., 2022. Mitochondrial characteristics of chicken breast muscle affected by wooden breast. Comp. Biochem. Physiol. a Mol. Integr. Physiol. 273, 111296.
Hinnebusch, A.G., 2006. eIF3: a versatile scaffold for translation initiation complexes. Trends. Biochem. Sci. 31, 553–562.
Horvath, S., 2011. Networks and fundamental concepts. Weighted Network Analysis. Springer, New York, NY.
Hosotani, M., Kawasaki, T., Hasegawa, Y., Wakasa, Y., Hoshino, M., Takahashi, N., Ueda, H., Takaya, T., Iwasaki, T., Watanabe, T., 2020. Physiological and pathological mitochondrial clearance is related to pectoralis major muscle pathogenesis in broilers with wooden breast syndrome. Front. Physiol. 11, 579.

Huang, D.W., Sherman, B..T., Lempicki, R.A., 2008. Systematic and integrative analysis of large gene lists using DAVID bioinformatics resources. Nat. Protoc. 4, 44–57.
Jackson, R.J., Hellen, C.U.T., Pestova, T.V., 2010. The mechanism of eukaryotic translation initiation and principles of its regulation. Nat. Rev. Mol. Cell Biol. 11, 113–127.
Karczewski, K.J., Snyder, M.P., 2018. Integrative omics for health and disease. Nat. Rev. Genet. 19, 299–310.
Kaur, J., Reinhardt, D.P., 2015. Extracellular matrix (ECM) molecules. Stem Cell Biology and Tissue Engineering in Dental Sciences. Academic press, pp. 25–45.
Kuttappan, V.A., Owens, C..M., Coon, C., Hargis, B.M., Vazquez-A Non, M., 2017. Research Note incidence of broiler breast myopathies at 2 different ages and its impact on selected raw meat quality parameters. Poult. Sci. 96, 3005–3009.
Lake, J.A., Dekkers, J.C.M., Abasht, B., 2021. Genetic basis and identification of candidate genes for wooden breast and white striping in commercial broiler chickens. Sci. Rep. 11, 1–13.
Langfelder, P., Horvath, S., 2008. WGCNA: an R package for weighted correlation network analysis. BMC. Bioinformatics. 9, 599.
Li, D., Wang, Y., Wang, J., Tang, Q., 2024. Identification of key proteins in early-onset Alzheimer's disease based on WGCNA. Front. Aging Neurosci. 16, 1412222.
Lin, B., Govindan, S., Lee, K., Zhao, P., Han, R., Runte, K.E., Craig, R., Palmer, B.M., Sadayappan, S., 2013. Cardiac myosin binding protein-C plays no regulatory role in skeletal muscle structure and function. PLoS. One 8, e69671.
Liu, J., Puolanne, E., Schwartzkopf, M., Arner, A., 2020. Altered sarcomeric structure and function in woody breast myopathy of avian Pectoralis major muscle. Front. Physiol. 11, 287.
McNamara, J.W., Sadayappan, S., 2018. Skeletal myosin binding protein-C: an increasingly important regulator of striated muscle physiology. Arch. Biochem. Biophys. 660, 121.
Mimaki, M., Wang, X., McKenzie, M., Thorburn, D.R., Ryan, M.T., 2012. Understanding mitochondrial Complex I assembly in health and disease. Biochim. Biophys. Acta 1817, 851–862.
Mlecnik, B., Galon, J., Bindea, G., 2018. Comprehensive functional analysis of large lists of genes and proteins. J. Proteomics. 171, 2–10.
Muona, A., Eklund, L., Väisänen, T., Pihlajaniemi, T., 2002. Developmentally regulated expression of type XV collagen correlates with abnormalities in Col15a1−/− mice. Matrix. Biol. 21, 89–102.
Mutryn, M.F., Brannick, E..M., Fu, W., Lee, W.R., Abasht, B., 2015. Characterization of a novel chicken muscle disorder through differential gene expression and pathway analysis using RNA-sequencing. BMC. Genomics. 16, 399.
Nice, E.C., 2022. The status of proteomics as we enter the 2020s: towards personalised/precision medicine. Anal. Biochem. 644, 113840.
Oulas, A., Minadakis, G., Zachariou, M., Sokratous, K., Bourdakou, M.M., Spyrou, G.M., 2019. Systems bioinformatics: increasing precision of computational diagnostics and therapeutics through network-based approaches. Brief. Bioinform. 20, 806–824.
Padilha, S.F., Ibelli, A.M.G., Peixoto, J.O., Cantão, M.E., Moreira, G.C.M., Fernandes, L. T., Tavernari, F.C., Morés, M.A.Z., Bastos, A.P.A., Dias, L.T., Teixeira, R.A., Ledur, M. C., 2024. Novel candidate genes involved in an initial stage of white striping development in broiler chickens. Animals 14, 2379.
Pampouille, E., Berri, C., Boitard, S., Hennequet-Antier, C., Beauclercq, S.A., Godet, E., Praud, C., Jégo, Y., Le Bihan-Duval, E., 2018. Mapping QTL for white striping in relation to breast muscle yield and meat quality traits in broiler chickens. BMC. Genomics. 19, 202.
Pampouille, E., Hennequet-Antier, C., Praud, C., Juanchich, A., Brionne, A., Godet, E., Bordeau, T., Fagnoul, F., Le Bihan-Duval, E., Berri, C., 2019. Differential expression and co-expression gene network analyses reveal molecular mechanisms and candidate biomarkers involved in breast muscle myopathies in chicken. Sci. Rep. 9, 14905.
Papah, M.B., Brannick, E..M., Schmidt, C.J., Abasht, B., 2017. Evidence and role of phlebitis and lipid infiltration in the onset and pathogenesis of wooden breast disease in modern broiler chickens. Avian Pathol. 46, 623–643.
Papah, M.B., Brannick, E..M., Schmidt, C.J., Abasht, B., 2018. Gene expression profiling of the early pathogenesis of wooden breast disease in commercial broiler chickens using RNA-sequencing. PLoS. One 3, e0207346.
Pei, G., Chen, L., Zhang, W., 2017. WGCNA application to proteomic and metabolomic data analysis. Meth. Enzym. 585, 135–158.
Petracci, M., Soglia, F., Madruga, M., Carvalho, L., Ida, E., Estévez, M., 2019. Wooden-breast, white striping, and spaghetti meat: causes, consequences and consumer perception of emerging broiler meat abnormalities. Compr. Rev. Food Sci. Food Saf. 18, 565–583.
Pollard, T.D., Beltzner, C.C., 2002. Structure and function of the Arp2/3 complex. Curr. Opin. Struct. Biol. 12, 768–774.
Praud, C., Jimenez, J., Pampouille, E., Couroussé, N., Godet, E., Le Bihan-Duval, E., Berri, C., 2020. Molecular phenotyping of white striping and wooden breast myopathies in chicken. Front. Physiol. 11, 633.
R Core Team, 2020. R: a Language and Environment for Statistical Computing. R Foundation for Statistical Computing, Vienna, Austria. Accessed December 2025. https://www.R-project.org/.
Rosati, D., Palmieri, M., Brunelli, G., Morrione, A., Iannelli, F., Frullanti, E., Giordano, A., 2024. Differential gene expression analysis pipelines and bioinformatic tools for the identification of specific biomarkers: a review. Comput. Struct. Biotechnol. J. 23, 1154–1168.
Sha, Z., Brill, L.M., Cabrera, R., Kleifeld, O., Scheliga, J.S., Glickman, M.H., Chang, E.C., Wolf, D.A., 2009. The eIF3 interactome reveals the translasome, a supercomplex linking protein synthesis and degradation machineries. Mol. Cell 36, 141–152.
Shannon, P., Markiel, A., Ozier, O., Baliga, N.S., Wang, J.T., Ramage, D., Amin, N., Schwikowski, B., Ideker, T., 1971. Cytoscape: a software environment for integrated models. Genome Res. 13, 426.
Sherman, B.T., Hao, M.., Qiu, J., Jiao, X., Baseler, M.W., Lane, H.C., Imamichi, T., Chang, W., 2022. DAVID: a web server for functional enrichment analysis and functional annotation of gene lists (2021 update). Nucleic. Acids. Res. 50, W216.
Simpson, S., Rutland, P., Rutland, C.S., 2017. Genomic insights into cardiomyopathies: a comparative cross-species review. Vet. Sci. 4, 19.
Soglia, F., Petracci, M., Davoli, R., Zappaterra, M., 2021. A critical review of the mechanisms involved in the occurrence of growth-related abnormalities affecting broiler chicken breast muscles. Poult. Sci. 100, 101180.
Soglia, F., Bordini, M., Mazzoni, M., Zappaterra, M., Di Nunzio, M., Clavenzani, P., Davoli, R., Meluzzi, A., Sirri, F., Petracci, M., 2022. The evolution of vimentin and desmin in pectoralis major muscles of broiler chickens supports their essential role in muscle regeneration. Front. Physiol. 13, 1839.
Song, T., Landim-Vieira, M., Ozdemir, M., Gott, C., Kanisicak, O., Pinto, J.R., Sadayappan, S., 2023. Etiology of genetic muscle disorders induced by mutations in fast and slow skeletal MyBP-C paralogs. Exp. Mol. Med. 55, 502.
Stancill, J.S., Corbett, J.A., 2022. Hydrogen peroxide detoxification through the peroxiredoxin/thioredoxin antioxidant system: a look at the pancreatic β-cell oxidant defense. Vitam. Horm. 121, 45.
Støle, T.P., Romaine, A.., Kleiberg, T., Høst, V., Lunde, M., Hasic, A., Lintvedt, T.A., Sanden, K.W., Kolset, S.O., Wold, J.P., Pisconti, A., Rønning, S.B., Carlson, C.R., Pedersen, M.E., 2025. Cardiac implications of chicken wooden breast myopathy. Front. Physiol. 16, 1547661.
Tasoniero, G., Cullere, M., Cecchinato, M., Puolanne, E., Dalle Zotte, A., 2016. Technological quality, mineral profile, and sensory attributes of broiler chicken breasts affected by White Striping and Wooden Breast myopathies. Poult. Sci. 95, 2707–2714.
Tasoniero, G., Zhuang, H., Gamble, G.R., Bowker, B.C., 2020. Effect of spaghetti meat abnormality on broiler chicken breast meat composition and technological quality. Poult. Sci. 99, 1724–1733.
Velleman, S.G., Clark, D.L., 2015. Histopathologic and myogenic gene expression changes associated with wooden breast in broiler breast muscles. Avian Dis. 59, 410–418.
Velleman, S.G., Clark, D..L., Tonniges, J.R., 2017. The effect of the wooden breast myopathy on sarcomere structure and organization. Avian Dis. 62, 28–35.
Velleman, S.G., 2002. Role of the extracellular matrix in muscle growth and development. J. Anim. Sci. 80, E8–E13.
Velleman, S.G., 2020. Pectoralis major (breast) muscle extracellular matrix fibrillar collagen modifications associated with the wooden breast fibrotic myopathy in broilers. Front. Physiol. 11, 461.
Velleman, S.G., 2023. Broiler breast muscle myopathies: association with satellite cells. Poult. Sci. 102, 102917.
Wang, Z., Brannick, E., Abasht, B., 2023a. Integrative transcriptomic and metabolomic analysis reveals alterations in energy metabolism and mitochondrial functionality in broiler chickens with wooden breast. Sci. Rep. 13, 4747.
Wang, C., Che, S., Susta, L., Barbut, S., 2023b. Textural and physical properties of breast fillets with myopathies (wooden breast, white striping, spaghetti meat) in Canadian fast-growing broiler chickens. Poult. Sci. 102, 102309.
Wang, Y., Li, B., Jian, C., Gagaoua, M., Estévez, M., Puolanne, E., Ertbjerg, P., 2025. Oxidative stress-induced changes in wooden breast and mitigation strategies: a review. Compr. Rev. Food Sci. Food Saf. 24, e70148.
Wei, W., Xu, J., Xing, C., Wang, H., Zhang, H., Liu, Y., He, X., Wang, J., Guo, X., Jiang, R., 2024. Identification of key module and hub genes affecting broiler body weight through weighted gene co-expression network analysis. Poult. Sci. 103, 104111.
Wolf, D.A., Lin, Y.., Duan, H., Cheng, Y., 2020. eIF-three to Tango: emerging functions of translation initiation factor eIF3 in protein synthesis and disease. J. Mol. Cell Biol. 12, 403.
Xing, T., Zhao, X., Zhang, L., Li, J.L., Zhou, G.H., Xu, X.L., Gao, F., 2020. Characteristics and incidence of broiler chicken wooden breast meat under commercial conditions in China. Poult. Sci. 99, 620–628.
Xing, T., Pan, X., Zhang, L., Gao, F., 2021. Hepatic oxidative stress, apoptosis, and inflammation in broiler chickens with wooden breast myopathy. Front. Physiol. 12, 415.
Xu, H., Wang, Z., Wang, Y., Pan, S., Zhao, W., Chen, M., Chen, X., Tao, T., Ma, L., Ni, Y., Li, W., 2023. GSTM2 alleviates heart failure by inhibiting DNA damage in cardiomyocytes. Cell Biosci. 13, 220.
Yasuda, M., Koshida, S., Sato, N., Obinata, T., 1995. Complete primary structure of chicken cardiac c-protein (MyBP-C) and its expression in developing striated muscles. J. Mol. Cell Cardiol. 27, 2275–2286.
Zambonelli, P., Zappaterra, M., Soglia, F., Petracci, M., Sirri, F., Cavani, C., Davoli, R., 2016. Detection of differentially expressed genes in broiler pectoralis major muscle affected by White Striping - Wooden Breast myopathies. Poult. Sci. 95, 2771–2785.
Zhang, Q., Ma, C., Gearing, M., Wang, P.G., Chin, L.S., Li, L., 2018. Integrated proteomics and network analysis identifies protein hubs and network alterations in Alzheimer's disease. Acta Neuropathol. Commun. 6, 19.
Zhang, W., Liu, Y., Zhang, H., 2021. Extracellular matrix: an important regulator of cell functions and skeletal muscle development. Cell Biosci. 11, 65.
Zhang, X., Xing, T., Zhao, L., Zhang, L., Gao, F., 2024. Transcriptomic meta-analysis and exploration of differentially expressed gene functions in wooden breast myopathy of broilers. Poult. Sci. 103, 104047.

Zhao, D., Song, Z., Shen, L., Xia, T., Ouyang, Q., Zhang, H., He, X., Kang, K., 2024. Single-cell transcriptomics and tissue metabolomics uncover mechanisms underlying wooden breast disease in broilers. Poult. Sci. 103, 104433.

Zhou, Z., Liu, J., Liu, J., 2024. Application of weighted gene co-expression network analysis to metabolomic data from an ApoA-I knockout mouse model. Molecules. 29, 694.

Zhou, H., Quach, A., Nair, M., Abasht, B., Kong, B., Bowker, B., 2025. Omics based technology application in poultry meat research. Poult. Sci. 104, 104643.